

---

# A simple higher-order beam model that is represented by two kinematic variables and three section constants

Hart Honickman<sup>1</sup> and Stefan Kloppenborg<sup>2</sup>

Journal Title  
XX(X):1–32  
©The Author(s) 2020  
Reprints and permission:  
sagepub.co.uk/journalsPermissions.nav  
DOI: 10.1177/ToBeAssigned  
www.sagepub.com/

SAGE

## Abstract

This manuscript presents a new higher-order beam model. The present beam model is governed by differential equations that are similar to those present in some existing higher-order beam models; however, the present beam model makes use of a novel method of calculating the transverse shear stiffness, which facilitates the calculation of a shear-warping stiffness without the need for an assumed warping displacement field, and without introducing any additional kinematic variables. The present beam model also facilitates the recovery of the distributions of longitudinal normal stresses and transverse shear stresses. The authors postulate that the bending and shear terms in first-order shear deformation theory represent the first two terms in an infinite series that would constitute an ideal one-dimensional beam model, and it is suggested that the present beam model constitutes the first four terms in this hypothetical infinite series. The present beam model is solved for several example beams, and the results are compared to those of existing classical and higher-order beam models, as well as computational results from finite element analyses. It is shown that the present beam model is able to accurately represent deformed shapes and stress distributions pertaining to beams that exhibit non-trivial shear compliance as well as non-trivial shear-warping stiffness. In the case of laminated composite beams comprising a large number of laminae, the present beam model offers a level of analytical fidelity that is comparable to that of existing zigzag beam models; however, unlike zigzag beam models, the present beam model is equally well suited for the analyses of beams comprising any number of laminae.

## Keywords

Beam, Transverse Shear, Shear deformation theory, Warping, Timoshenko, Zigzag, Saint-Venant, Laminate, Composite

## 1 Introduction

Despite the continual advancement of the finite element method and other computational modeling techniques, classical one-dimensional beam models continue to enjoy extensive use within the academic and industrial sectors. Perhaps the most commonly known classical one-dimensional beam models are Euler-Bernoulli beam theory and Timoshenko beam theory<sup>1,2</sup>.

Euler-Bernoulli beam theory assumes a relationship between an applied transverse load and the resulting deflection. In Euler-Bernoulli beam theory, the applied transverse shear force produces a bending moment, which produces a curvature dependent on the flexural (bending) stiffness of the beam. This curvature is then successively integrated to obtain transverse deflections. Timoshenko beam theory<sup>1,2</sup> improves upon this relationship by accounting for additional transverse compliance caused by shear deformations. In essence, Timoshenko beam theory is an early example of first-order shear deformation theory. First-order shear deformation theories (such as Timoshenko beam theory) typically manifest themselves as the super-position of bending deflections and shear deflections, and are dependent upon knowledge of material properties, geometric properties, and derived section constants that represent

---

<sup>1</sup>Shinc Inc., Toronto, Ontario, Canada, <https://orcid.org/0000-0002-8140-0676>

<sup>2</sup>Comtek Advanced Structures Ltd., Burlington, Ontario, Canada, <https://orcid.org/0000-0002-1908-5214>

### Corresponding author:

Hart Honickman, Shinc Inc. 505 Glenlake Avenue, Toronto, Ontario, M6P 1G9, Canada.  
Email: [hart@shinc.ca](mailto:hart@shinc.ca)

the mechanical characteristics of the beam. The required properties and section constants for first-order shear deformation theories typically include longitudinal elastic moduli, shear moduli, second area moments of inertia, cross-sectional areas, and shear correction factors.

Timoshenko beam theory (and other first-order shear deformation theories) has earned a great deal of attention among academic researchers. Some researchers have focused on characterizing the capabilities and limitations of Timoshenko beam theory, and have highlighted some paradoxes that are present within the boundary conditions that must be imposed<sup>3 4</sup>. A particularly large amount of effort has been focused on determining an ideal shear correction factor for use with Timoshenko beam theory<sup>5</sup>. Researchers have proposed elasticity-based formulations<sup>6</sup> and energy-based formulations<sup>7</sup> for the calculation of a shear correction factor. In recent years, numerous researchers have developed high fidelity computational and semi-analytical methods that employ analyses of the sectional warping displacement field in order to calculate each of the section constants that are required for use with Timoshenko beam theory (including the shear correction factor); these computational and semi-analytical methods have included the variational asymptotic beam sectional analysis (VABS) method<sup>8 9 10</sup>, the semi-analytical finite element (SAFE) method<sup>11 12 13 14</sup>, and a plethora of other similar and related works<sup>15 16 17 18 19</sup>.

It is generally understood that many of the limitations of first-order shear deformation theories (such as Timoshenko beam theory) stem from their inability to account for the effects of non-uniform warping of the beam section<sup>20 4</sup>. Some researchers have attempted to overcome the inherent limitations of first-order shear deformation theories by opting to develop higher-order shear deformation theories, such as third-order shear deformation theories, that endeavor to account for non-uniform warping of the cross-sections of beams and plates<sup>21 22 20 23</sup>. Unfortunately, the cubic warping displacement field that is assumed by third-order shear deformation theories causes erroneous results for beams that exhibit heterogeneous compositions; this problem is particularly evident in the context of laminated composite beams and plates<sup>24</sup>. As such, some researchers have developed layer-wise theories of beams and plates, wherein the kinematics of each layer (lamina) within a laminate are independently defined, and the layer-to-layer continuity of some physical parameters is enforced<sup>25 26</sup>. In order to overcome the relatively high computational expense of layer-wise theories, some researchers have developed so-called “zigzag” models, wherein the sectional warping displacement fields of laminated composite beams and plates are approximated by piecewise linear functions<sup>27 25 28</sup>. In general, the mathematical bases of these zigzag models are not inherently well suited to the analyses of homogeneous beams or laminated beams comprising a small number of thick homogeneous laminae; however, the so-called “Homogeneous Limit Methodology for Zigzag Function Selection” (HLMZFS) has been developed as a means to extend the applicability of zigzag models to the analyses of such beams<sup>24</sup>. The HLMZFS is based upon the notion that any homogeneous layer of rectangular cross-section can be partitioned into many laminae, and then small perturbations can be applied to the mechanical properties of the material that is present within each of said laminae, thereby simulating the existence of a pseudo-heterogeneous laminate and, in turn, facilitating the application of a zigzag model. The perturbations applied to the shear modulus of each of the laminae follow a parabolic distribution through the depth of the beam, thus achieving a parabolic shear stress distribution, as is expected in a homogeneous beam. Unfortunately, the HLMZFS is dependent upon ad-hoc decisions pertaining to the number of laminae that should be used and the magnitude of the perturbations that should be applied to the mechanical properties of the materials that are present within said laminae. Additionally, in a beam comprising multiple dissimilar materials, the perturbations applied in the HLMZFS model are negligible in comparison with the actual differences in mechanical properties of the beam, thus the model effectively reverts to a standard zigzag model, and piecewise constant shear stresses are predicted.

Linear sandwich theory<sup>29 30</sup> is a method of modelling the elastic response of laminated composite sandwich panels, while accounting for the effects of non-uniform warping of the cross-section. In essence, linear sandwich theory can be likened to a special case simplification of zigzag models, wherein a simple sectional warping displacement field can be assumed on the basis of the unique characteristics of laminated composite sandwich panels.

The so-called “Carrera Unified Formulation” (CUF)<sup>31 32 33 34 35</sup> is a computational method, wherein the order of the model may be stipulated as a solution control parameter. CUF models are not bound by any specific pre-determined displacement functions; as such, CUF beam analyses may be configured to mimic (or improve upon) the behaviour of Euler-Bernoulli beam theory, Timoshenko beam theory, third-order shear deformation theory, or higher-order shear deformation theories. Ultimately, CUF can be likened to a computationally-efficient substitute for three-dimensional finite element analysis. Unfortunately, practical implementation of CUF requires a considerably greater commitment than some of the other analytical methods that have been discussed herein. While CUF has many desirable attributes,

it is unlikely that an industry engineer would adopt the use of CUF for a single-use (one-off) application if said engineer was not already accustomed to using CUF.

Engineers often have a need to rapidly correlate experimental test results (such as material qualification test results) with analytical predictions. For example, aerospace engineers frequently engage in rigorous material characterization test programs that often include a plethora of small-scale experimental transverse loading tests (such as 3-point bending tests or 4-point bending tests); by correlating these experimental test results with analytical predictions, engineers are often able to semi-empirically derive engineering constants that are needed for subsequent engineering efforts, as well as achieve a more comprehensive understanding of the experimental observations. Some composite laminates that are used in aerospace applications (particularly those that include one or more constrained layers of an elastomeric material) exhibit non-trivial transverse shear compliance coupled with non-trivial shear-warping stiffness. The transverse displacement of these laminates cannot be accurately predicted by simple Euler-Bernoulli or Timoshenko beam models; however, high-fidelity three-dimensional finite element analyses are often regarded as being too cumbersome and time consuming to be considered for this type of application. As such, there continues to exist a need for high-fidelity analytical beam models that can quickly and easily be implemented by industry engineers who are accustomed to writing simple bespoke computer software scripts or spreadsheets.

In the present manuscript, a new one-dimensional beam model is presented. This new beam model is governed by differential equations that are similar to those present in some existing higher-order beam models; however, the new beam model is unique in the means by which the required section constants are calculated. The present beam model makes use of a novel method of calculating the transverse shear stiffness; this transverse shear stiffness facilitates the calculation of a shear-warping stiffness that is formulated based upon fundamental elasticity relationships, without the need for an assumed warping displacement field. Furthermore, the shear-warping stiffness is calculated without introducing any additional kinematic variables to the governing equations of the beam model: the differential equations governing the model are second-order in both transverse displacement and rotation, with no additional kinematic variables. The resulting shear-warping stiffness remains accurate for heterogeneous material compositions, and is therefore applicable to laminated composite beams. The present beam model also facilitates the recovery of the distributions of longitudinal normal stresses and transverse shear stresses at all positions within the beam. The present beam model may be implemented using a simple bespoke computer software script or spreadsheet.

## 2 Background

The present discussion uses an orthogonal Cartesian coordinate system defined by the three axes:  $x$ ,  $y$ , and  $z$ , where the longitudinal axis of the undeformed beam is initially parallel to the  $x$ -axis. In general, the terms “section” and “cross-section” are used herein in reference to  $y$ - $z$  cross-sectional planes that are established prior to deformation of a beam; after the beam has deformed, said sections may become non-planar (due to warping displacements) and may translate and rotate relative to their initial states. Each beam section has a local  $y$ - $y$  axis that is parallel to the global  $y$ -axis. While all of the beam theories discussed herein are applicable to any direction of transverse loading, in the interest of clarity, the authors have elected to discuss beams in the context of transverse shear forces that act parallel to the  $z$ -axis, coupled with moments that act about the  $y$ - $y$  axis of the beam section ( $y$ - $y$  moments). As such, it is assumed that all applied loads act parallel to the  $z$ -axis. In general, the term “elevation” is used herein in reference to positions and dimensions that are measured parallel to the  $z$ -axis. The term “longitudinal elastic modulus” herein denotes the Young’s modulus of elasticity measured parallel to the  $x$ -axis.

In the case of a linear elastic beam, Timoshenko beam theory<sup>1,2</sup> can be represented by a system of two coupled differential equations, which express the bending moment and the transverse shear force in terms of the transverse deflection and the rotation of the cross-sectional plane at any  $x$  position along the length of the beam. The first of these differential equations expresses the  $y$ - $y$  moment at any  $x$  position along the length of the beam, as follows:

$$M_{yy\text{Timoshenko}} = -EI_{yy} \frac{d\phi_{yy}}{dx} \quad (1)$$

where  $M_{yy\text{Timoshenko}}$  is the moment about the  $y$ - $y$  axis of the beam section;  $EI_{yy}$  is the flexural (bending) stiffness of the beam section about its  $y$ - $y$  axis, based upon the assumption that bending strains vary linearly along the  $z$ -axis (Euler-Bernoulli assumptions); and  $\phi_{yy}$  is the angle of rotation of the section at position  $x$  about its  $y$ - $y$  axis, measured relative to the initial undeformed shape of the beam. The second of the aforementioned two differential equations expresses the transverse shear force at any  $x$  position along the length of the beam, as follows:

$$V_{z\text{Timoshenko}} = \kappa_z AG_{xz} \left( \frac{dw}{dx} - \phi_{yy} \right) \quad (2)$$

where  $V_{z\text{Timoshenko}}$  is a transverse shear force applied parallel to the  $z$ -axis;  $w$  is the transverse deflection of the beam in the  $z$  direction, measured relative to the initial undeformed shape of the beam;  $AG_{xz}$  is the area integral of local  $x$ - $z$  shear moduli over the entire  $y$ - $z$  cross-sectional area of the beam; and  $\kappa_z$  is the shear correction factor for use with transverse shear forces that are applied parallel to the  $z$ -axis. In the case of Timoshenko beam theory, it is assumed that the product of  $\kappa_z$  and  $AG_{xz}$  represents the transverse shear stiffness of the beam section, for use with transverse shear forces that are applied parallel to the  $z$ -axis.

It is evident from equations (1) and (2) that the governing equations of Timoshenko beam theory include two kinematic variables:  $w$  and  $\phi_{yy}$ . Since  $\phi_{yy}$  represents the true angle of rotation of the section at position  $x$ , whereas  $\frac{dw}{dx}$  represents the slope of the longitudinal axis of the deformed beam at position  $x$ , any difference between these values represents a shear angle (herein referred to as a “nominal shear angle”) that is measured within the  $x$ - $z$  plane of the beam.

Figure 1 shows the deformed shape of a transversely loaded beam, and helps to illustrate some of the geometric dimensions that are relevant to Timoshenko beam theory, as well as the present beam model.

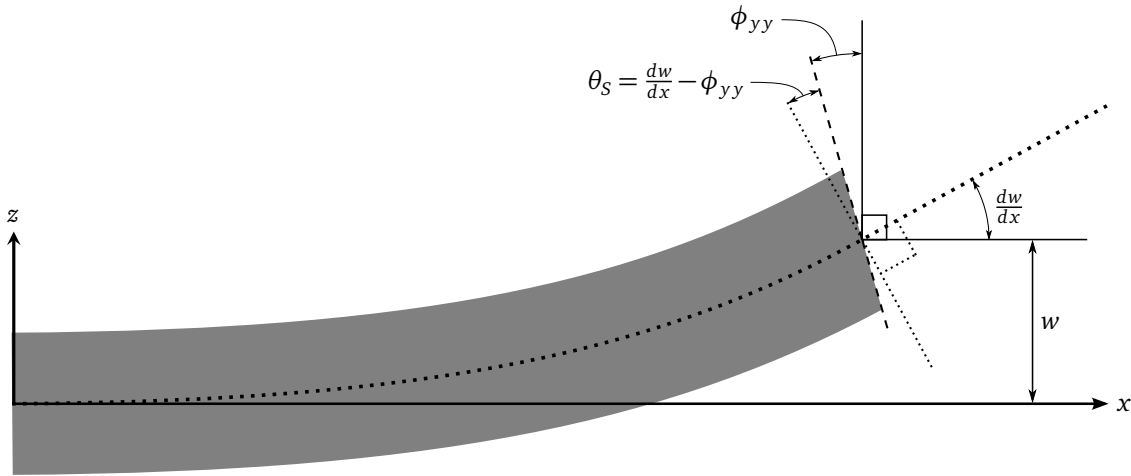


**Figure 1.** Deformed shape of a transversely loaded beam, illustrating some of the geometric dimensions that are relevant to Timoshenko beam theory, as well as the present beam model

### 3 Governing Equations of the Present Beam Model

The present beam model constitutes an extension of Timoshenko beam theory that endeavors to account for resistance to variations in transverse shear deformations along the length of the beam. In order to facilitate this provision, it is convenient to define a nominal shear angle,  $\theta_s$ , as follows:

$$\theta_s = \frac{dw}{dx} - \phi_{yy} \quad (3)$$

With this definition for  $\theta_s$ , the total curvature of the beam can be expressed (for cases where  $w$  is small in relation to the size of the beam), as follows:

$$\text{Curvature} = \frac{d^2w}{dx^2} \left[ 1 + \left( \frac{dw}{dx} \right)^2 \right]^{-3/2} \approx \frac{d^2w}{dx^2} = \frac{d\phi_{yy}}{dx} + \frac{d\theta_s}{dx} \quad (4)$$

It is important to note that, in the context of the cross-sectional plane of the beam, positive rotations of  $\phi_{yy}$  and  $\theta_s$  occur in opposite directions. Conversely, in the context of the apparent slope of the deflected beam within the  $x$ - $z$

plane, positive rotations of  $\phi_{yy}$  and  $\theta_S$  occur in the same direction. This apparent discrepancy is an artifact of the definition of engineering shear strain angles.

In order to maximize ease of exposition of the present beam model, the differential equation for moments about the  $y$ - $y$  axis will be decomposed into two components:  $M_{yyB}$  and  $M_{yyW1}$ . These two components of the moment will later be added by superposition. Similarly, the differential equation for transverse shear forces that act parallel to the  $z$ -axis will be decomposed into two components:  $V_{zB}$  and  $V_{zW1}$ . These two components of the transverse shear force will later be added by superposition.

The first component of the moment,  $M_{yyB}$ , is identical to that which exists in both Euler-Bernoulli and Timoshenko beam theories, and is expressed as follows:

$$M_{yyB} = -EI_{yy} \frac{d\phi_{yy}}{dx} \quad (5)$$

A detailed derivation of equation (5) is included in Section 4.2.

Differentiating  $M_{yyB}$  with respect to  $x$  gives an expression for the component of the transverse shear force due to bending, denoted by  $V_{zB}$ , as follows:

$$V_{zB} = -\frac{dEI_{yy}}{dx} \frac{d\phi_{yy}}{dx} - EI_{yy} \frac{d^2\phi_{yy}}{dx^2} \quad (6)$$

In the context of a beam that exhibits constant cross-sectional geometry and composition along its length, equation (6) can be simplified, as follows:

$$V_{zBc} = -EI_{yy} \frac{d^2\phi_{yy}}{dx^2} \quad (7)$$

It will be shown in Section 4.3 that  $V_{zBc}$  can be expressed in terms of  $\theta_S$ , as follows:

$$V_{zBc} = -EI_{yy} \frac{d^2\phi_{yy}}{dx^2} = \Lambda_{xz} \theta_S \quad (8)$$

where  $\Lambda_{xz}$  is the transverse shear stiffness of the beam section, for use with transverse shear forces that are applied parallel to the  $z$ -axis. In the context of the present beam model, the value of  $\Lambda_{xz}$  is calculated in accordance with the method that is described in Section 4.3.

Up to this point, it should be evident to the reader that the present beam model is equivalent to Timoshenko beam theory (with the exception of the method by which the transverse shear stiffness is calculated), since equation (5) is equivalent to equation (1), and equation (8) is equivalent to equation (2).

As will be shown in Sections 4.3 and 4.4, the very existence of equation (8) indicates that plane sections do not remain planar in any case where transverse shear forces are non-zero, thus invalidating one of the assumptions that was employed in the formulation of equation (5). In order to compensate for this erroneous assumption, it is possible to add a term to the moment equation that serves to account for additional moments (shear-warping moments) that are generated due to the rate of change of shear-warping displacements with respect to  $x$ , where shear-warping displacements are longitudinal warping displacements that are caused by transverse shear strains. As will be shown in Sections 4.3 and 4.4, this shear-warping moment term,  $M_{yyW1}$ , can be expressed as follows:

$$M_{yyW1} = -\beta_{1z} \frac{d\theta_S}{dx} \quad (9)$$

where  $\beta_{1z}$  is a stiffness term that relates the rate of change of  $\theta_S$  with respect to  $x$  to the generation of some additional moment (shear-warping moment). In essence,  $\beta_{1z}$  is a stiffness term that describes the resistance of the beam to longitudinal non-uniformity of the shear-warping displacements of its section. As such, it is fitting to refer to  $\beta_{1z}$  as a shear-warping stiffness. The subscripts in the notation for  $\beta_{1z}$  are representative of the fact that this term relates to moments that are generated as a function of the first derivative of nominal shear angles with respect to  $x$ , wherein said nominal shear angles are caused by transverse shear forces that act parallel to the  $z$ -axis.

Summing equations (5) and (9), the overall moment about the  $y$ - $y$  axis of the beam section can now be expressed, as follows:

$$M_{yy} = M_{yyB} + M_{yyW1} = -EI_{yy} \frac{d\phi_{yy}}{dx} - \beta_{1z} \frac{d\theta_S}{dx} \quad (10)$$

where  $M_{yy}$  is the total moment about the  $y$ - $y$  axis of the beam section. Differentiating  $M_{yy}$  with respect to  $x$  gives the following more complete expression for the transverse shear force:

$$V_z = -\frac{dEI_{yy}}{dx} \frac{d\phi_{yy}}{dx} - EI_{yy} \frac{d^2\phi_{yy}}{dx^2} - \frac{d\beta_{1z}}{dx} \frac{d\theta_S}{dx} - \beta_{1z} \frac{d^2\theta_S}{dx^2} \quad (11)$$

where  $V_z$  is the total transverse shear force applied parallel to the  $z$ -axis. With reference to equation (11), it is convenient to decompose  $V_z$  into two components, as follows:

$$V_z = V_{zB} + V_{zW1} \quad (12)$$

where:

$$V_{zW1} = -\frac{d\beta_{1z}}{dx} \frac{d\theta_S}{dx} - \beta_{1z} \frac{d^2\theta_S}{dx^2} \quad (13)$$

From inspection of equations (12), (6), and (13), it is evident that  $V_{zB}$  represents the component of the transverse shear force that is caused by variations in  $\phi_{yy}$  along the length of the beam, whereas  $V_{zW1}$  represents the component of the transverse shear force that is caused by variations in  $\theta_S$  along the length of the beam.

In the context of a beam that exhibits constant cross-sectional geometry and composition along its length, equation (12) can be simplified, as follows:

$$V_{zC} = V_{zBC} + V_{zW1C} \quad (14)$$

where:

$$V_{zW1C} = -\beta_{1z} \frac{d^2\theta_S}{dx^2} \quad (15)$$

$V_{zC}$  is equivalent to  $V_z$  when the cross-sectional geometry and composition are held constant. Similarly,  $V_{zBC}$  is equivalent to  $V_{zB}$  when the cross-sectional geometry and composition are held constant, and  $V_{zW1C}$  is equivalent to  $V_{zW1}$  when the cross-sectional geometry and composition are held constant.

Substituting equations (8) and (15) into equation (14) gives the following expression for  $V_{zC}$ :

$$V_{zC} = \Lambda_{xz} \theta_S - \beta_{1z} \frac{d^2\theta_S}{dx^2} \quad (16)$$

Ultimately, the present beam model is embodied by equations (10) and (16) (where equation (16) represents the amalgamation of equations (14), (8), and (15)). In long regions of a beam within which transverse shear forces are approximately constant, the nominal shear angle will also be approximately constant (in accordance with Saint-Venant's principle<sup>36</sup>), and equations (10) and (16) will effectively simplify to equations (1) and (2), respectively.

The governing equations of the present beam model (equations (10) and (16)) include two kinematic variables:  $\phi_{yy}$  and  $\theta_S$ . With reference to equation (3), it is evident that the kinematic variables in the present beam model are equivalent to those present in Timoshenko beam theory. It is interesting to note that the governing equations of the present beam model (equations (10) and (16)) are quite similar to the governing equations of linear sandwich theory<sup>29,30</sup>; however, it will be shown herein that the present beam model is not limited to the analysis of sandwich panels.

From inspection of equations (10) and (16), it is evident that  $V_{zC}$  is only dependent upon  $\theta_S$ , whereas  $M_{yy}$  is dependent upon both  $\phi_{yy}$  and  $\theta_S$ . As such, in the context of a statically determinate structure, where  $M_{yy}$  and  $V_{zC}$  are both known over the entire length of the beam, it is convenient to solve equation (16) first (either analytically or computationally). Once equation (16) has been solved, the resulting  $\theta_S$  distribution can be substituted into equation (10) in order to solve for  $\phi_{yy}$ . Once  $\phi_{yy}$  and  $\theta_S$  have both been determined, the overall curvature profile of the beam can be calculated using equation (4), and the deflected shape of the beam can then be determined by carrying out successive integrations of the calculated curvature profile.

## 4 Section Constants for the Present Beam Model

### 4.1 General

In the interest of clarity and ease of exposition, the section constants for the present beam model are derived herein in the context of the following simplifying assumptions:

1. It is assumed that the beam constitutes a laminated composite beam wherein each ply comprises a linear elastic orthotropic material having three orthogonal symmetry planes, and wherein the surface normal of each of said symmetry planes is aligned with one of the  $x$ - $y$ - $z$  coordinate axes of the beam.
2. It is assumed that the beam exhibits a constant rectangular cross-sectional geometry and composition along its length, thus significantly simplifying the derivation of the section constants by facilitating the use of equations (14), (8), (15), and (16).
3. It is assumed that all stresses act parallel to the  $x$ - $z$  plane; as such, the effects of Poisson's ratio are neglected.
4. It is assumed that all normal strains and normal stresses act parallel to the longitudinal axis of the beam; as such, the effects of Poisson's ratio are neglected.

Notwithstanding the foregoing, readers who are skilled in the art will appreciate that the spirit and philosophy embodied by the following derivations for section constants can be applied to higher fidelity formulations that account for general anisotropy, as well as the effects of full three-dimensional mechanical phenomena. In fact, the authors believe that the general philosophy of the derivations presented herein could be executed (with increased fidelity) by one or more of the many computational or semi-analytical methods that have been shown in the literature<sup>8 9 10 11 12 13 14 15 16 17 18 19</sup> to be effective for the calculation of the section constants of beams.

### 4.2 Flexural Stiffness

For the purpose of calculating the flexural stiffness,  $EI_{yy}$ , of the beam, it is assumed that plane sections remain planar after deformation, and longitudinal bending displacements vary linearly along the  $z$ -axis (Euler-Bernoulli beam assumptions), as follows:

$$u_B = -(Z - Z_{NA}) \phi_{yy} \quad (17)$$

where  $Z$  is the elevation coordinate of some specific point of interest within the beam section, measured with respect to the bottom surface of the beam;  $Z_{NA}$  is the elevation of the  $y$ - $y$  flexural neutral axis of the beam section, measured with respect to the bottom surface of the beam; and  $u_B$  is the longitudinal bending displacement (measured parallel to the  $x$ -axis), evaluated at elevation  $Z$ .

Differentiating  $u_B$  with respect to  $x$ , the longitudinal ( $x$ ) bending strain,  $\epsilon_{xB}$ , can be expressed at elevation  $Z$ , as follows:

$$\epsilon_{xB} = \frac{du_B}{dx} = -(Z - Z_{NA}) \frac{d\phi_{yy}}{dx} \quad (18)$$

The longitudinal ( $x$ ) bending stress,  $\sigma_{xB}$ , can now be expressed at elevation  $Z$ , as follows:

$$\sigma_{xB} = -E_{xx} (Z - Z_{NA}) \frac{d\phi_{yy}}{dx} \quad (19)$$

where  $E_{xx}$  is the longitudinal elastic modulus of the material present at elevation  $Z$ .

Integrating bending stresses over the cross-sectional area of the beam, the total longitudinal force,  $F_B$ , that is generated as a result of bending stresses can be expressed as follows:

$$F_B = \int_{Z=Z_B}^{Z_T} B \sigma_{xB} dZ \quad (20)$$

where  $Z_B$  and  $Z_T$  are the elevations of the bottom and top surfaces of the entire beam section, respectively, each measured with respect to the bottom surface of the beam; and  $B$  is the total width of the beam section, measured

parallel to the  $y$ -axis. Substituting equation (19) into equation (20) and setting  $F_B$  equal to zero for pure bending, the following expression can be written:

$$0 = \frac{d\phi_{yy}}{dx} \int_{Z=Z_B}^{Z_T} B E_{xx} (Z - Z_{NA}) dZ \quad (21)$$

The value of  $Z_{NA}$  can then be determined by solving the integral in equation (21) and rearranging the resulting expression to isolate for  $Z_{NA}$ , as follows:

$$Z_{NA} = \frac{\int_{Z=Z_B}^{Z_T} Z B E_{xx} dZ}{\int_{Z=Z_B}^{Z_T} B E_{xx} dZ} \quad (22)$$

At this point, it is convenient to introduce a new elevation variable,  $\zeta$ , as follows:

$$\zeta = Z - Z_{NA} \quad (23)$$

From inspection of equation (23), it is evident that  $\zeta$  represents an elevation coordinate measured with respect to the  $y$ - $y$  flexural neutral axis of the beam section.

The bending moment within the beam due to bending curvatures alone (ignoring the effects of transverse shear) can be expressed as follows:

$$M_{yyB} = -\frac{d\phi_{yy}}{dx} \int_{\zeta=\zeta_B}^{\zeta_T} B E_{xx} \zeta^2 d\zeta \quad (24)$$

where  $\zeta_B$  is the elevation of the bottom surface of the entire beam section, measured with respect to the  $y$ - $y$  flexural neutral axis of the beam section;  $\zeta_T$  is the elevation of the top surface of the entire beam section, measured with respect to the  $y$ - $y$  flexural neutral axis of the beam section; and  $E_{xx}$  is the longitudinal elastic modulus of the material present at elevation  $\zeta$ .

Substituting equation (5) into equation (24) and rearranging the resulting formula, the flexural stiffness of the beam section can be calculated as follows:

$$EI_{yy} = \int_{\zeta=\zeta_B}^{\zeta_T} B E_{xx} \zeta^2 d\zeta \quad (25)$$

### 4.3 Transverse Shear Stiffness

Unfortunately, many of the existing methods for calculating the transverse shear stiffness of a beam section would result in shear-warping displacement fields that fail to satisfy a work-energy balance between shear-warping moments and the corresponding longitudinal warping strains. In the context of first-order shear deformation theories, this may not be problematic because warping deformations are ignored by such beam theories. Conversely, in the context of higher-order beam theories that endeavor to account for the effects of shear-warping, the aforementioned work-energy balance must be achieved.

The present beam model employs a novel formulation for the calculation of the transverse shear stiffness of the beam section,  $A_{xz}$ , which ensures that work that is done by local shear-warping moments is balanced by the corresponding local strain energy that is associated with the longitudinal warping strain field.

The  $x$ - $z$  shear strain at each elevation within a beam's cross-section can be expressed as a function of the rate of change of bending curvature along the length of the beam, as follows:

$$\gamma_{xzB} = \frac{1}{B G_{xz}} \left( \int_{\zeta=\zeta_B}^{\zeta_h} B E_{xx} \zeta d\zeta \right) \frac{d^2 \phi_{yy}}{dx^2} \quad (26)$$

where  $\zeta_h$  is some specific elevation of interest within the beam section, measured with respect to the  $y$ - $y$  flexural neutral axis of the beam section;  $\gamma_{xzB}$  is the  $x$ - $z$  shear strain that is caused solely by the rate of change of bending curvatures, evaluated at elevation  $\zeta_h$ ;  $E_{xx}$  is the longitudinal elastic modulus of the material present at elevation  $\zeta$ ; and  $G_{xz}$  is the  $x$ - $z$  shear modulus of the material present at elevation  $\zeta_h$ .

Substituting equation (8) into equation (26), the following expression is found:

$$\gamma_{xzB} = \frac{\Lambda_{xz} \theta_S}{EI_{yy} B G_{xz}} \left( - \int_{\zeta=\zeta_B}^{\zeta_h} B E_{xx} \zeta d\zeta \right) \quad (27)$$

It is convenient to define a new term,  $Q_V$ , as the integral of the first moment of longitudinal elastic moduli about the  $y$ - $y$  flexural neutral axis of the beam section, for all material below elevation  $\zeta_h$ , as follows:

$$Q_V = - \int_{\zeta=\zeta_B}^{\zeta_h} B E_{xx} \zeta d\zeta \quad (28)$$

where  $E_{xx}$  is the longitudinal elastic modulus of the material present at elevation  $\zeta$ . Substituting  $Q_V$  into equation (27), the formula for  $\gamma_{xzB}$  can be rewritten as follows:

$$\gamma_{xzB} = \frac{\Lambda_{xz} Q_V}{EI_{yy} B G_{xz}} \theta_S \quad (29)$$

where  $G_{xz}$  is the  $x$ - $z$  shear modulus of the material present at elevation  $\zeta_h$ .

It is useful to define  $\gamma_{xzBRel}$  as the difference between  $\gamma_{xzB}$  (the actual  $x$ - $z$  transverse shear strain angle) and  $\theta_S$  (the nominal shear angle) at elevation  $\zeta_h$ , as follows:

$$\gamma_{xzBRel} = \frac{\Lambda_{xz} Q_V}{EI_{yy} B G_{xz}} \theta_S - \theta_S \quad (30)$$

The shear-warping displacement,  $u_{W1}$ , can be defined as the longitudinal displacement (measured parallel to the  $x$ -axis) that is caused solely by  $x$ - $z$  transverse shear strains. At some specific elevation within the beam section,  $\zeta_H$ , the shear-warping displacement can be expressed as follows:

$$u_{W1} = \int_{\zeta_h=\zeta_B}^{\zeta_H} \gamma_{xzBRel} d\zeta_h + u_{W1B} \quad (31)$$

where  $\zeta_H$  is some specific elevation of interest within the beam section, measured with respect to the  $y$ - $y$  flexural neutral axis of the beam section; and  $u_{W1B}$  represents the longitudinal shear-warping displacement (measured parallel to the  $x$ -axis) at the bottom surface of the beam (where  $\zeta_h = \zeta_B$ ). Since all values of  $u_{W1}$  (including the value of  $u_{W1}$  evaluated at  $\zeta_h = \zeta_B$ ) are dependent upon the nominal shear angle,  $\theta_S$ , it is convenient to express  $u_{W1B}$  as the product of  $\theta_S$  and some constant,  $C_{uW1}$ , as follows:

$$u_{W1B} = C_{uW1} \theta_S \quad (32)$$

It is now possible to express the longitudinal ( $x$ ) normal strain,  $\epsilon_{xW1}$ , that is caused solely by a rate of change of  $\theta_S$  along the length of the beam, at elevation  $\zeta_H$ , as follows:

$$\epsilon_{xW1} = \frac{du_{W1}}{dx} \quad (33)$$

In the interest of solving equation (33), it is convenient to define a new term,  $R_{W1}$ , as follows:

$$R_{W1} = \int_{\zeta_h=\zeta_B}^{\zeta_H} \frac{Q_V}{B G_{xz}} d\zeta_h \quad (34)$$

where  $G_{xz}$  is the  $x$ - $z$  shear modulus of the material present at elevation  $\zeta_h$ .

Having defined  $R_{W1}$ , equation (33) can now be rewritten, as follows:

$$\varepsilon_{xW1} = \frac{d\theta_S}{dx} \left( \frac{\Lambda_{xz}}{EI_{yy}} R_{W1} - [\zeta_H + Z_{NA}] + C_{uW1} \right) \quad (35)$$

where  $[\zeta_H + Z_{NA}]$  represents the distance between elevation  $\zeta_H$  and the bottom surface of the beam.

The term  $F_{xW1}$  denotes the total longitudinal force that is generated within the beam as a result of  $\varepsilon_{xW1}$ ; the value of  $F_{xW1}$  can be expressed as follows:

$$F_{xW1} = \int_{\zeta_H=\zeta_B}^{\zeta_T} \varepsilon_{xW1} B E_{xx} d\zeta_H \quad (36)$$

where  $E_{xx}$  is the longitudinal elastic modulus of the material present at elevation  $\zeta_H$ . For a beam that is only undergoing transverse loading, the value of  $F_{xW1}$  must be equal to zero. As such, substituting equation (35) into equation (36), and setting  $F_{xW1} = 0$ , the following expression is found:

$$0 = \frac{d\theta_S}{dx} \int_{\zeta_H=\zeta_B}^{\zeta_T} \left( \frac{\Lambda_{xz}}{EI_{yy}} R_{W1} - [\zeta_H + Z_{NA}] + C_{uW1} \right) B E_{xx} d\zeta_H \quad (37)$$

The value of  $C_{uW1}$  can be expressed in terms of  $\Lambda_{xz}$  and  $EI_{yy}$  by solving the integral in equation (37) and rearranging the resulting expression to isolate for  $C_{uW1}$ , as follows:

$$C_{uW1} = C_{W1C} + \frac{\Lambda_{xz}}{EI_{yy}} C_{W11} \quad (38)$$

where:

$$C_{W1C} = \frac{\int_{\zeta_H=\zeta_B}^{\zeta_T} (\zeta_H + Z_{NA}) B E_{xx} d\zeta_H}{\int_{\zeta_H=\zeta_B}^{\zeta_T} B E_{xx} d\zeta_H}$$

$$C_{W11} = \frac{- \int_{\zeta_H=\zeta_B}^{\zeta_T} R_{W1} B E_{xx} d\zeta_H}{\int_{\zeta_H=\zeta_B}^{\zeta_T} B E_{xx} d\zeta_H}$$

Once the values of  $C_{W1C}$  and  $C_{W11}$  have been determined, it is possible to express the total internal longitudinal ( $x$ ) normal strain energy that is generated as a result of the rate of change of shear deformation along the length of the beam, per unit length of beam,  $dx$ , as follows:

$$\frac{dU_{intW1\varepsilon}}{dx} = \frac{1}{2} \int_{\zeta_H=\zeta_B}^{\zeta_T} \varepsilon_{xW1}^2 B E_{xx} d\zeta_H \quad (39)$$

Substituting equations (35) and (38) into equation (39) gives the following expression:

$$\frac{dU_{intW1\varepsilon}}{dx} = \frac{1}{2} \left( \frac{d\theta_S}{dx} \right)^2 \beta_{1Uint} \quad (40)$$

where:

$$\beta_{1Uint} = \int_{\zeta_H=\zeta_B}^{\zeta_T} \left( \frac{\Lambda_{xz}}{EI_{yy}} [R_{W1} + C_{W11}] - \zeta_H - Z_{NA} + C_{W1C} \right)^2 B E_{xx} d\zeta_H \quad (41)$$

where  $E_{xx}$  is the longitudinal elastic modulus of the material present at elevation  $\zeta_H$ .

The moment due to warping strains can be determined by integrating the moments of the corresponding stresses about the  $y$ - $y$  flexural neutral axis of the beam section, as follows:

$$M_{yyW1} = \int_{\zeta_H=\zeta_B}^{\zeta_T} \varepsilon_{xW1} \zeta_H B E_{xx} d\zeta_H \quad (42)$$

where  $M_{yyW1}$  is the additional moment (shear-warping moment) that is necessary in order to facilitate variations in the nominal shear angle,  $\theta_S$ , along the length of the beam. If  $M_{yyW1}$  were equal to zero, then the value of  $\theta_S$  would be constant.  $M_{yyW1}$  is present in equation (9). Substituting equations (35) and (38) into equation (42) gives the following expression:

$$M_{yyW1} = -\beta_{1Uext} \frac{d\theta_S}{dx} \quad (43)$$

where:

$$\beta_{1Uext} = - \int_{\zeta_H=\zeta_B}^{\zeta_T} \left( \frac{\Lambda_{xz}}{EI_{yy}} [R_{W1} + C_{W11}] - \zeta_H - Z_{NA} + C_{W1C} \right) \zeta_H B E_{xx} d\zeta_H \quad (44)$$

where  $E_{xx}$  is the longitudinal elastic modulus of the material present at elevation  $\zeta_H$ . The external work that corresponds to  $M_{yyW1}$  can be expressed, per unit length of beam,  $dx$ , as follows:

$$\frac{dU_{extW1\varepsilon}}{dx} = -\frac{1}{2} M_{yyW1} \frac{d\theta_S}{dx} \quad (45)$$

Substituting equation (43) into equation (45) gives the following expression:

$$\frac{dU_{extW1\varepsilon}}{dx} = \frac{1}{2} \left( \frac{d\theta_S}{dx} \right)^2 \beta_{1Uext} \quad (46)$$

Recognizing that external work due to shear-warping moments must be equal to internal strain energy due to the corresponding sectional warping, it follows that equation (46) must be equal to equation (40). Upon setting equation (46) equal to equation (40), it is evident that the values of  $\beta_{1Uint}$  and  $\beta_{1Uext}$  must be equal to each other. As such, the value of  $\Lambda_{xz}$  can be solved by setting the expression for  $\beta_{1Uint}$  (equation (41)) equal to the expression for  $\beta_{1Uext}$  (equation (44)), and rearranging the resulting equation in order to isolate  $\Lambda_{xz}$ . In order to achieve this, it is convenient to first express  $\beta_{1Uint}$  and  $\beta_{1Uext}$  in terms of  $\Lambda_{xz}$ , as follows:

$$\beta_{1Uint} = P_{\beta C} + P_{\beta 1} \Lambda_{xz} + P_{\beta 2} \Lambda_{xz}^2 \quad (47)$$

$$\beta_{1Uext} = N_{\beta C} + N_{\beta 1} \Lambda_{xz} \quad (48)$$

where  $P_{\beta C}$ ,  $P_{\beta 1}$ ,  $P_{\beta 2}$ ,  $N_{\beta C}$ , and  $N_{\beta 1}$  are section constants that may be calculated as follows:

$$P_{\beta C} = \int_{\zeta_H=\zeta_B}^{\zeta_T} (C_{W1C} - \zeta_H - Z_{NA})^2 B E_{xx} d\zeta_H \quad (49)$$

$$P_{\beta 1} = \frac{1}{EI_{yy}} \int_{\zeta_H=\zeta_B}^{\zeta_T} 2(R_{W1} + C_{W11})(C_{W1C} - \zeta_H - Z_{NA}) B E_{xx} d\zeta_H \quad (50)$$

$$P_{\beta 2} = \frac{1}{(EI_{yy})^2} \int_{\zeta_H=\zeta_B}^{\zeta_T} (R_{W1} + C_{W11})^2 B E_{xx} d\zeta_H \quad (51)$$

$$N_{\beta C} = - \int_{\zeta_H=\zeta_B}^{\zeta_T} (C_{W1C} - \zeta_H - Z_{NA}) \zeta_H B E_{xx} d\zeta_H \quad (52)$$

$$N_{\beta 1} = \frac{-1}{EI_{yy}} \int_{\zeta_H=\zeta_B}^{\zeta_T} (R_{W1} + C_{W11}) \zeta_H B E_{xx} d\zeta_H \quad (53)$$

where  $E_{xx}$  is the longitudinal elastic modulus of the material present at elevation  $\zeta_H$ .

Setting  $\beta_{1U_{int}}$  equal to  $\beta_{1U_{ext}}$  and finding the roots of the resulting quadratic formula, the value of  $\Lambda_{xz}$  can be calculated as follows:

$$\Lambda_{xz} = \frac{[4P_{\beta 2}(N_{\beta C} - P_{\beta C}) + (N_{\beta 1} - P_{\beta 1})^2]^{1/2} + N_{\beta 1} - P_{\beta 1}}{2P_{\beta 2}} \quad (54)$$

It is worth emphasizing, as mentioned previously, that many existing methods for calculating the transverse shear stiffness of a beam section would result in shear-warping displacement fields that fail to satisfy a work-energy balance between shear-warping moments and the corresponding longitudinal warping strains. For example, one may be inclined to attempt to find a value of  $\Lambda_{xz}$  by employing the ‘‘directional shear energy’’ method that is used to find shear correction factors in<sup>5</sup> (a modified version of the method presented in<sup>7</sup>): this would give values of  $\Lambda_{xz}$  that, when substituted into equations (43) and (44), yield shear-warping moments of approximately zero. Paradoxically, these same values of  $\Lambda_{xz}$  yield non-zero values of warping strain energy when they are substituted into equations (40) and (41). This inconsistency prompted the present authors to develop the present formulation for  $\Lambda_{xz}$ .

#### 4.4 Resistance to Variations in Shear Angle

Recall from equation (9) that the shear-warping moment,  $M_{yyW1}$ , is expressed as follows:

$$M_{yyW1} = -\beta_{1z} \frac{d\theta_S}{dx} \quad (55)$$

Recognizing that equation (55) is equivalent to equation (43), it is now evident that the value of  $\beta_{1z}$  is equal to the value of  $\beta_{1U_{ext}}$ . As such, the value of  $\beta_{1z}$  may be calculated as follows:

$$\beta_{1z} = \beta_{1U_{ext}} = N_{\beta C} + N_{\beta 1} \Lambda_{xz} \quad (56)$$

Recalling that  $\beta_{1U_{ext}}$  is equal to  $\beta_{1U_{int}}$ , it is also possible to calculate the value of  $\beta_{1z}$  as follows:

$$\beta_{1z} = \beta_{1U_{int}} = P_{\beta C} + P_{\beta 1} \Lambda_{xz} + P_{\beta 2} \Lambda_{xz}^2 \quad (57)$$

From inspection of the preceding derivation, it is evident that  $\beta_{1z}$  essentially represents the resistance of the beam’s section to a rate of change of  $\theta_S$  with respect to  $x$ , wherein each local value of  $\theta_S$  corresponds to a local shear-warping displacement field. As such, it is fitting to refer to  $\beta_{1z}$  as a shear-warping stiffness.

Differentiating  $M_{yyW1}$  with respect to  $x$ , it is possible to find a transverse shear force,  $V_{zW1}$ , that corresponds to  $M_{yyW1}$ , as follows:

$$V_{zW1} = \frac{dM_{yyW1}}{dx} \quad (58)$$

Substituting equation (55) into equation (58), the following expression for  $V_{zW1}$  is found:

$$V_{zW1} = -\frac{d\beta_{1z}}{dx} \frac{d\theta_S}{dx} - \beta_{1z} \frac{d^2\theta_S}{dx^2} \quad (59)$$

In the context of a beam that exhibits constant cross-sectional geometry and composition along its length, equation (59) can be simplified as follows:

$$V_{zW1c} = -\beta_{1z} \frac{d^2\theta_S}{dx^2} \quad (60)$$

$V_{zW1c}$  represents the additional transverse shear force that is necessary in order to facilitate variations in the nominal shear angle,  $\theta_S$ , along the length of the beam. If  $V_{zW1c}$  were equal to zero, then the value of  $\theta_S$  would be constant.  $V_{zW1c}$  is present in equations (14) and (15).

It is evident that equations (55) and (60) are identical to equations (9) and (15), respectively, thus concluding the derivation of the present beam model.

#### 4.5 Section Constants for a Laminated Composite Beam

In the context of a laminated composite beam, equation (22) for  $Z_{NA}$  can be solved as follows:

$$Z_{NA} = \frac{\sum_{k=1}^n [E_{xxk} (Z_{tk}^2 - Z_{bk}^2)]}{2 \sum_{k=1}^n [E_{xxk} (Z_{tk} - Z_{bk})]} \quad (61)$$

where  $Z_{bk}$  is the value of  $Z$  at the bottom of lamina  $k$ ,  $Z_{tk}$  is the value of  $Z$  at the top of lamina  $k$ ,  $E_{xxk}$  is the longitudinal elastic modulus of the material that is present within lamina  $k$ , and  $n$  is the total number laminae (plies) in the laminate.

In the context of a laminated composite beam, equation (25) for  $EI_{yy}$  can be solved as follows:

$$EI_{yy} = \frac{B}{3} \sum_{k=1}^n [E_{xxk} (\zeta_{tk}^3 - \zeta_{bk}^3)] \quad (62)$$

where  $\zeta_{bk}$  is the value of  $\zeta$  at the bottom of lamina  $k$ , and  $\zeta_{tk}$  is the value of  $\zeta$  at the top of lamina  $k$ .

In the context of a laminated beam, equation (28) for  $Q_V$  can be solved at any elevation within each lamina  $k$  as follows:

$$Q_{Vk} = - \int_{\zeta=\zeta_{bk}}^{\zeta_h} B E_{xxk} \zeta d\zeta - \sum_{i=1}^{k-1} \int_{\zeta=\zeta_{bi}}^{\zeta_{ti}} B E_{xxi} \zeta d\zeta \quad (63)$$

where  $Q_{Vk}$  is the value of  $Q_V$ , evaluated at some elevation,  $\zeta_h$ , that resides within lamina  $k$ ;  $\zeta_{bi}$  and  $\zeta_{ti}$  are the values of  $\zeta$  at the bottom and top of lamina  $i$ , respectively; and  $E_{xxi}$  is the longitudinal elastic modulus of the material that is present within lamina  $i$ . The definite integrals for  $Q_{Vk}$  can be solved within their integration bounds as follows:

$$Q_{Vk} = \frac{-B E_{xxk}}{2} (\zeta_h^2 - \zeta_{bk}^2) - \sum_{i=1}^{k-1} \left[ \frac{B E_{xxi}}{2} (\zeta_{ti}^2 - \zeta_{bi}^2) \right] \quad (64)$$

It should be noted that the value of  $Q_{Vk}$  can be evaluated at any elevation within the thickness of lamina  $k$ ; however, the equations describing  $Q_{Vk}$  are unique within each lamina. As such,  $Q_{Vk}$  is calculated as a piecewise summation

of the definite integrals though the thicknesses of each lamina below the elevation of interest, and up to the exact elevation of interest,  $\zeta_h$ , which resides somewhere within the thickness of lamina  $k$ . For practical purposes, it is more convenient to expand  $Q_{V_k}$  into the following polynomial:

$$Q_{V_k} = A_{Ck} + A_{2k} \zeta_h^2 \quad (65)$$

where:

$$A_{Ck} = \frac{B}{2} \left\{ E_{xxk} \zeta_{bk}^2 - \sum_{i=1}^{k-1} [E_{xxi} (\zeta_{ti}^2 - \zeta_{bi}^2)] \right\}$$

$$A_{2k} = \frac{-B E_{xxk}}{2}$$

In the context of a laminated composite beam, equation (34) for  $R_{W1}$  may be evaluated at any elevation within each lamina  $k$  as follows:

$$R_{W1k} = \int_{\zeta_h=\zeta_B}^{\zeta_H} \frac{Q_V}{B G_{xzk}} d\zeta_h = D_{Ck} + D_{1k} \zeta_H + D_{3k} \zeta_H^3 \quad (66)$$

where:

$$D_{Ck} = \frac{1}{B} \left\{ -\frac{A_{Ck}}{G_{xzk}} \zeta_{bk} - \frac{A_{2k}}{3G_{xzk}} \zeta_{bk}^3 + \sum_{i=1}^{k-1} \left[ \frac{A_{Ci}}{G_{xzi}} (\zeta_{ti} - \zeta_{bi}) + \frac{A_{2i}}{3G_{xzi}} (\zeta_{ti}^3 - \zeta_{bi}^3) \right] \right\}$$

$$D_{1k} = \frac{A_{Ck}}{B G_{xzk}}$$

$$D_{3k} = \frac{A_{2k}}{3B G_{xzk}}$$

where  $R_{W1k}$  is the value of  $R_{W1}$ , evaluated at some elevation,  $\zeta_H$ , that resides within lamina  $k$ ;  $A_{Ci}$  and  $A_{2i}$  have the same definitions as  $A_{Ck}$  and  $A_{2k}$ , respectively, but are evaluated within lamina  $i$  instead of lamina  $k$ ; and  $G_{xzi}$  and  $G_{xzk}$  are the  $x$ - $z$  shear moduli of the materials that are present within laminae  $i$  and  $k$ , respectively.

In the context of a laminated composite beam, the values of  $C_{W1C}$  and  $C_{W11}$  can be calculated by solving the definite integrals in equation (38), as follows:

$$C_{W1C} = \frac{\sum_{k=1}^n \left\{ E_{xxk} \left[ Z_{NA} (\zeta_{tk} - \zeta_{bk}) + \frac{1}{2} (\zeta_{tk}^2 - \zeta_{bk}^2) \right] \right\}}{\sum_{k=1}^n \left\{ E_{xxk} (\zeta_{tk} - \zeta_{bk}) \right\}} \quad (67)$$

$$C_{W11} = \frac{\sum_{k=1}^n \left\{ E_{xxk} \left[ -D_{Ck} (\zeta_{tk} - \zeta_{bk}) - \frac{1}{2} D_{1k} (\zeta_{tk}^2 - \zeta_{bk}^2) - \frac{1}{4} D_{3k} (\zeta_{tk}^4 - \zeta_{bk}^4) \right] \right\}}{\sum_{k=1}^n \left\{ E_{xxk} (\zeta_{tk} - \zeta_{bk}) \right\}} \quad (68)$$

In the context of a laminated composite beam, the values of  $P_{\beta C}$ ,  $P_{\beta 1}$ ,  $P_{\beta 2}$ ,  $N_{\beta C}$ , and  $N_{\beta 1}$  may be calculated by solving equations (49), (50), (51), (52), and (53), as follows:

$$P_{\beta C} = B \sum_{k=1}^n \left\{ E_{xxk} \left[ (Z_{NA} - C_{W1C})^2 (\zeta_{tk} - \zeta_{bk}) \right. \right. \\ \left. \left. + (Z_{NA} - C_{W1C}) (\zeta_{tk}^2 - \zeta_{bk}^2) \right. \right. \\ \left. \left. + \frac{1}{3} (\zeta_{tk}^3 - \zeta_{bk}^3) \right] \right\} \quad (69)$$

$$\begin{aligned}
P_{\beta 1} = \frac{B}{EI_{yy}} \sum_{k=1}^n \left\{ E_{xxk} \left[ 2(C_{W1C} - Z_{NA})(D_{Ck} + C_{W11})(\zeta_{tk} - \zeta_{bk}) \right. \right. \\
+ [D_{1k}(C_{W1C} - Z_{NA}) - D_{Ck} - C_{W11}](\zeta_{tk}^2 - \zeta_{bk}^2) \\
- \frac{2}{3}D_{1k}(\zeta_{tk}^3 - \zeta_{bk}^3) \\
+ \frac{1}{2}D_{3k}(C_{W1C} - Z_{NA})(\zeta_{tk}^4 - \zeta_{bk}^4) \\
\left. \left. - \frac{2}{5}D_{3k}(\zeta_{tk}^5 - \zeta_{bk}^5) \right] \right\} \quad (70)
\end{aligned}$$

$$\begin{aligned}
P_{\beta 2} = \frac{B}{(EI_{yy})^2} \sum_{k=1}^n \left\{ E_{xxk} \left[ (D_{Ck} + C_{W11})^2(\zeta_{tk} - \zeta_{bk}) \right. \right. \\
+ D_{1k}(D_{Ck} + C_{W11})(\zeta_{tk}^2 - \zeta_{bk}^2) \\
+ \frac{1}{3}D_{1k}^2(\zeta_{tk}^3 - \zeta_{bk}^3) \\
+ \frac{1}{2}D_{3k}(D_{Ck} + C_{W11})(\zeta_{tk}^4 - \zeta_{bk}^4) \\
+ \frac{2}{5}D_{1k}D_{3k}(\zeta_{tk}^5 - \zeta_{bk}^5) \\
\left. \left. + \frac{1}{7}D_{3k}^2(\zeta_{tk}^7 - \zeta_{bk}^7) \right] \right\} \quad (71)
\end{aligned}$$

$$\begin{aligned}
N_{\beta C} = -B \sum_{k=1}^n \left\{ E_{xxk} \left[ \frac{1}{2}(C_{W1C} - Z_{NA})(\zeta_{tk}^2 - \zeta_{bk}^2) \right. \right. \\
\left. \left. - \frac{1}{3}(\zeta_{tk}^3 - \zeta_{bk}^3) \right] \right\} \quad (72)
\end{aligned}$$

$$\begin{aligned}
N_{\beta 1} = \frac{-B}{EI_{yy}} \sum_{k=1}^n \left\{ E_{xxk} \left[ \frac{1}{2}(D_{Ck} + C_{W11})(\zeta_{tk}^2 - \zeta_{bk}^2) \right. \right. \\
+ \frac{1}{3}D_{1k}(\zeta_{tk}^3 - \zeta_{bk}^3) \\
\left. \left. + \frac{1}{5}D_{3k}(\zeta_{tk}^5 - \zeta_{bk}^5) \right] \right\} \quad (73)
\end{aligned}$$

It is interesting to note that, in cases wherein the assumptions of linear sandwich theory are applicable, the preceding equations for the section constants of the present beam model will converge upon the section constants that are utilized in linear sandwich theory<sup>29 30</sup>.

## 5 Stress Analysis with the Present Beam Model

### 5.1 General

The initial impetus for the development of the present beam model was to achieve accurate displacement predictions for transversely loaded laminated composite beams having arbitrary material compositions. Notwithstanding the foregoing, the present beam model also facilitates the recovery of stress values.

## 5.2 Normal Stress

Substituting equation (23) into equation (19), the normal stress due to bending can be evaluated at elevation  $\zeta$ , as follows:

$$\sigma_{xB} = -\frac{d\phi_{yy}}{dx} E_{xx} \zeta \quad (74)$$

where  $E_{xx}$  is the longitudinal elastic modulus of the material present at elevation  $\zeta$ .

Recalling equation (35) for  $\varepsilon_{xW1}$ , the normal stress,  $\sigma_{xW1}$ , that is caused by a rate of change of nominal shear angle can be evaluated at elevation  $\zeta_H$ , as follows:

$$\sigma_{xW1} = \frac{d\theta_S}{dx} \left( \frac{\Lambda_{xz}}{EI_{yy}} R_{W1} - \zeta_H - Z_{NA} + C_{uW1} \right) E_{xx} \quad (75)$$

where  $E_{xx}$  is the longitudinal elastic modulus of the material present at elevation  $\zeta_H$ , and the value of  $C_{uW1}$  may be calculated using equation (38). The preceding expression for  $\sigma_{xW1}$  can be rewritten in the context of a laminated composite beam by substituting equation (66) into equation (75).

Finally, the total longitudinal ( $x$ ) normal stress,  $\sigma_x$ , can be determined at any position within the beam section by summing  $\sigma_{xB}$  and  $\sigma_{xW1}$ , as follows:

$$\sigma_x = \sigma_{xB} + \sigma_{xW1} \quad (76)$$

## 5.3 Shear Stress

Recalling equation (29) for  $\gamma_{xzB}$ , the shear stress,  $\tau_{xzB}$ , that is caused by a rate of change of bending curvatures can be evaluated at elevation  $\zeta_h$ , as follows:

$$\tau_{xzB} = \frac{\Lambda_{xz} Q_V}{EI_{yy} B} \theta_S \quad (77)$$

The preceding expression for  $\tau_{xzB}$  can be rewritten in the context of a laminated composite beam by substituting equation (65) into equation (77).

The shear stress,  $\tau_{xzW1}$ , that is caused by shear-warping can be evaluated at elevation  $\zeta_L$ , as follows:

$$\tau_{xzW1} = -\frac{1}{B} \int_{\zeta_H=\zeta_B}^{\zeta_L} \left( \frac{d\varepsilon_{xW1}}{dx} \right) B E_{xx} d\zeta_H \quad (78)$$

where  $\zeta_L$  is some specific elevation of interest within the beam section, measured with respect to the  $y$ - $y$  flexural neutral axis of the beam section;  $\tau_{xzW1}$  is evaluated at elevation  $\zeta_L$ ; and  $E_{xx}$  is the longitudinal elastic modulus of the material present at elevation  $\zeta_H$ . Substituting equation (35) into equation (78) gives the following expression for  $\tau_{xzW1}$ :

$$\tau_{xzW1} = -\frac{1}{B} \frac{d^2\theta_S}{dx^2} \int_{\zeta_H=\zeta_B}^{\zeta_L} \left( \frac{\Lambda_{xz}}{EI_{yy}} R_{W1} - \zeta_H - Z_{NA} + C_{uW1} \right) B E_{xx} d\zeta_H \quad (79)$$

where the value of  $C_{uW1}$  may be calculated using equation (38). In the context of a laminated composite beam, equation (79) can be solved as a piecewise definite integral, as follows:

$$\tau_{xzW1} = -\frac{d^2\theta_S}{dx^2} (T_{Ck} + T_{1k}\zeta_L + T_{2k}\zeta_L^2 + T_{4k}\zeta_L^4) \quad (80)$$

where:

$$\begin{aligned}
 T_{Ck} &= T_{CSk} - T_{1k}\zeta_{bk} - T_{2k}\zeta_{bk}^2 - T_{4k}\zeta_{bk}^4 \\
 T_{CSk} &= \sum_{i=1}^{k-1} [T_{1i}(\zeta_{ti} - \zeta_{bi}) + T_{2i}(\zeta_{ti}^2 - \zeta_{bi}^2) + T_{4i}(\zeta_{ti}^4 - \zeta_{bi}^4)] \\
 T_{1k} &= E_{xxk} \left( \frac{\Lambda_{xz}}{EI_{yy}} D_{Ck} - Z_{NA} + C_{uW1} \right) \\
 T_{2k} &= \frac{E_{xxk}}{2} \left( \frac{\Lambda_{xz}}{EI_{yy}} D_{1k} - 1 \right) \\
 T_{4k} &= \frac{E_{xxk}}{4} \left( \frac{\Lambda_{xz}}{EI_{yy}} D_{3k} \right)
 \end{aligned}$$

where the value of  $\tau_{xzW1}$  is evaluated at some elevation,  $\zeta_L$ , that resides within lamina  $k$ ; and  $T_{1i}$ ,  $T_{2i}$ , and  $T_{4i}$  have the same definitions as  $T_{1k}$ ,  $T_{2k}$ , and  $T_{4k}$ , respectively, but are evaluated within lamina  $i$  instead of lamina  $k$ .

Finally, the total  $x$ - $z$  shear stress can be determined at any position within the beam section by summing  $\tau_{xzB}$  and  $\tau_{xzW1}$ , as follows:

$$\tau_{xz} = \tau_{xzB} + \tau_{xzW1} \quad (81)$$

## 6 Increased Fidelity for the Present Beam Model

### 6.1 Additional Shear Compliance

Upon reviewing the derivation presented in Section 4.3, it is evident that  $\theta_S$  represents a nominal shear angle that corresponds to the shear strains that are described by equation (29); as such,  $\theta_S$  represents a nominal shear angle that corresponds to  $V_{zB_C}$  (see equation (8)). By extension, it is reasonable to hypothesize that there may also exist an additional nominal shear angle,  $\theta_{W1}$ , that corresponds to  $V_{zW1_C}$  (see equation (15)). From inspection of equation (79) for  $\tau_{xzW1}$ , it is evident that the shear strains that correspond to  $V_{zW1_C}$  may be expressed in terms of the second derivative of  $\theta_S$  with respect to  $x$ ; as such,  $\theta_{W1}$  can likely be defined as follows:

$$\theta_{W1} = C_{\theta W1} \frac{d^2 \theta_S}{dx^2} \quad (82)$$

where  $C_{\theta W1}$  is a section constant that can likely be calculated using a method that is analogous to the method that was used to calculate  $\Lambda_{xz}$  in Section 4.3. Differentiating  $\theta_{W1}$  with respect to  $x$  would give a corresponding additional shear curvature, which may be added to equation (4).

### 6.2 Higher-Order Terms

The shear-warping moment,  $M_{yyW1}$ , was introduced for the purpose of accounting for non-uniform sectional warping that is caused by the shear strains that are associated with  $V_{zB_C}$ . In like manner, there are also shear strains that are associated with  $V_{zW1_C}$ , which cause additional shear-warping displacements of the section; consequently, some additional shear-warping moment,  $M_{yyW3}$ , is generated as a function of the rate of change of these additional shear-warping displacements along the length of the beam. This additional shear-warping moment may be expressed as follows:

$$M_{yyW3} = \beta_{3z} \frac{d^3 \theta_S}{dx^3} \quad (83)$$

where  $\beta_{3z}$  is a stiffness term that relates the third derivative of  $\theta_S$  with respect to  $x$  to the generation of some additional moment (shear-warping moment) about the  $y$ - $y$  axis of the beam section. The subscripts in the notation for  $\beta_{3z}$  are representative of the fact that this term relates to moments that are generated as a function of the third derivative of nominal shear angles with respect to  $x$ , wherein said nominal shear angles are caused by transverse shear forces that act parallel to the  $z$ -axis. If  $M_{yyW3}$  were to be added to equation (10) and the resulting expression were to be differentiated with respect to  $x$ , an additional shear force component would result, as follows:

$$V_{zW3} = \frac{d\beta_{3z}}{dx} \frac{d^3\theta_S}{dx^3} + \beta_{3z} \frac{d^4\theta_S}{dx^4} \quad (84)$$

where  $V_{zW3}$  may be added to equation (12), equation (14), or equation (16). The shear strains that correspond to  $V_{zW3}$  may also cause an additional nominal shear angle,  $\theta_{W3}$ , which can likely be expressed as follows:

$$\theta_{W3} = C_{\theta W3} \frac{d^4\theta_S}{dx^4} \quad (85)$$

where it is assumed that  $\beta_{3z}$  is constant along  $x$ , and where  $C_{\theta W3}$  is a section constant that can likely be calculated using a method that is analogous to the method that was used to calculate  $\Lambda_{xz}$  in Section 4.3. Differentiating  $\theta_{W3}$  with respect to  $x$  would give a corresponding additional shear curvature, which may be added to equation (4).

At this point, the reader may appreciate that the aforementioned sequence can likely be repeated an infinite number of times. For each new shear-warping moment term that is added to the moment equation, another shear force component may be added to the transverse shear force equation. Similarly, for each new shear force component that is added to the transverse shear force equation, some additional shear-warping displacement field may be derived as a function of the corresponding shear strains, and a corresponding additional shear-warping moment term may be added to the moment equation. In addition, for each new shear force component that is added to the transverse shear force equation, an additional nominal shear angle may be defined, and a corresponding additional shear curvature component may be added to the total curvature equation (as proposed in Section 6.1). With each successive iteration through this cyclic derivation procedure, the resulting differential equations for moment and transverse shear force (the governing equations) will increase in order, thus offering improved analytical fidelity at the expense of increased mathematical complexity. In some respects, one can liken the aforementioned cyclic derivation procedure to a Taylor series, wherein each additional term brings the formula closer to an exact solution, but in the absence of an infinite number of terms, an exact solution is never achieved.

### 6.3 Practical Considerations

For the purpose of the present manuscript, the authors have elected to only account for the effects of the first shear-warping stiffness,  $\beta_{1z}$ , and neglect the effects of all higher-order warping effects. Furthermore, the authors have elected to only account for the effects of transverse shear compliance that is associated with  $\theta_S$ , and neglect the effects of nominal shear angles that may correspond to any other terms of the shear force equation. The authors believe that this model offers a good balance between fidelity and practicality for the case of most beams that exhibit non-trivial shear compliance. In particular, the authors believe that this model significantly improves upon Timoshenko beam theory by offering a solution that is devoid of discontinuities in the slope of the deflection profile, whereas Timoshenko beams theory yields a step change in slope (and a point of infinite curvature) anywhere that the beam is subjected to a step-change in transverse shear force.

Notwithstanding the foregoing, the authors encourage the reader to explore the hypotheses that were presented in Sections 6.1 and 6.2.

## 7 Boundary Conditions for the Present Beam Model

In Timoshenko beam theory, equations (2) and (3) can be combined to form an algebraic relationship between transverse shear force,  $V_{zTimoshenko}$ , and the nominal shear angle,  $\theta_S$ . This relationship can then be combined with equation (1) to produce a second-order differential equation relating moment,  $M_{yyTimoshenko}$ , and the transverse deflection,  $w$ . As such, to solve these equations for a statically determinant beam, two boundary conditions are required.

Equations (10) and (16) are the differential equations that give the deformed shape of the beam under the present beam theory. These equations are second-order differential equations in both  $\theta_S$  and  $w$ . Therefore, a total of four boundary conditions are required for a statically determinant beam.

Table 1 lists some common boundary conditions that are applicable to the present beam theory. The boundary condition for a free end warrants some discussion, however, as such a boundary condition is not always required for other beam theories.

At the free end, the longitudinal normal stress must be zero at all elevations, since no longitudinal forces act on the free end of the beam. Setting the longitudinal normal stresses to zero is equivalent to setting the longitudinal normal

strains to zero. Equations (18), (23), and (35) can be combined to obtain the total longitudinal normal strain at any elevation,  $\zeta_H$ , as follows:

$$\varepsilon_x = \varepsilon_{xB} + \varepsilon_{xW1} = -\zeta_H \frac{d\phi_{yy}}{dx} + \frac{d\theta_S}{dx} \left( \frac{\Lambda_{xz}}{EI_{yy}} R_{W1k} - \zeta_H - Z_{NA} + C_u W1 \right) \quad (86)$$

or, equivalently,

$$\varepsilon_x = -\zeta_H \left( \frac{d^2 w}{dx^2} - \frac{d\theta_S}{dx} \right) + \frac{d\theta_S}{dx} \left( \frac{\Lambda_{xz}}{EI_{yy}} R_{W1k} - \zeta_H - Z_{NA} + C_u W1 \right) \quad (87)$$

In order to set  $\varepsilon_x = 0$  at all elevations, the two conditions  $\frac{d^2 w}{dx^2} = 0$  and  $\frac{d\theta_S}{dx} = 0$  are necessary at the free end. However, at a free end, by definition, the moment,  $M_{yy}$ , is zero. In the present beam theory, the total moment is given by equation (10); therefore, setting  $M_{yy} = 0$  and also setting  $\frac{d\theta_S}{dx} = 0$  has the effect of also setting  $\frac{d\phi_{yy}}{dx} = 0$ , and with reference to equation (4), this also has the effect of setting  $\frac{d^2 w}{dx^2} = 0$ .

**Table 1.** Common boundary conditions for the present beam model

Physical Constraint	Boundary Condition at Location of Constraint
Roller (no transverse deflection)	$w = 0$
Guided (no rotation)	$\frac{dw}{dx} = 0$ and $\theta_S = 0$
Fixed (no transverse deflection, no rotation)	$w = 0$ , $\frac{dw}{dx} = 0$ , and $\theta_S = 0$
Free End	$\frac{d\theta_S}{dx} = 0$

## 8 Sample Analyses and Comparisons with Other Models

For demonstration purposes, the equations for the present beam theory have been solved for a number of example beams. The present manuscript is focused on the section constants and the governing equations of the present beam model. For these examples, the finite difference method was used to solve the equations; however, the authors expect that the finite element method or analytical methods could also be used to solve these equations. In these examples, a grid spacing of 0.03 mm, was used. The Python source code for the computer software that was used to solve the model is provided to the reader in an online archive<sup>37</sup>.

For demonstration purposes, a single beam loading configuration is presented. This beam has a total length of 36 mm, and is symmetrically supported by a pair of pin/roller supports that are positioned 24 mm apart. A single point load of 200 N is applied transversely (parallel to the z-axis) at the centre of the beam. Since the beam is symmetric about a plane containing the applied load, half of the beam has been analyzed with a symmetry condition imposed, as shown in Figure 2.

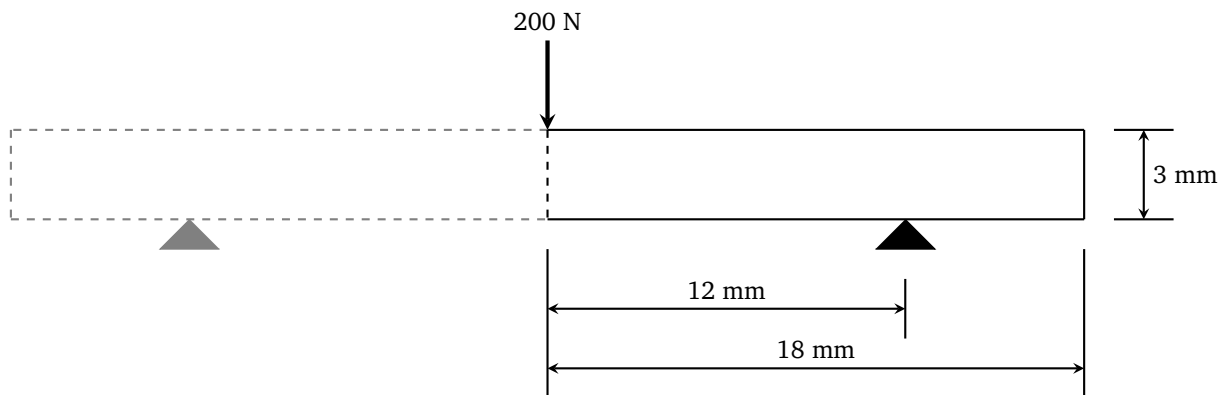


**Figure 2.** Loading configuration of the beam used in the present demonstration. Since the beam is symmetric, half the beam was analyzed with a symmetry condition imposed in the middle

Three beams, each comprising a unique laminate, are shown as examples here. Each beam has a width of 1 mm (measured parallel to the  $y$ -axis). Each laminate has a total thickness of 3 mm (measured parallel to the  $z$ -axis), and comprises three laminae that each have a thickness of 1 mm. The first laminate, denoted by “Laminate A”, comprises three identical laminae that are each composed of a typical unidirectional carbon fiber reinforced polymer having its fibers aligned with the longitudinal axis of the beam. The second laminate, denoted by “Laminate B”, comprises a lower lamina that is composed of a typical aluminium alloy, an upper lamina that is composed of the same material that is present within Laminate A, and an inner (core) lamina that is composed of a typical unidirectional carbon fiber reinforced polymer having its fibers oriented perpendicular to the longitudinal axis of the beam. The third laminate, denoted by “Laminate C”, comprises upper and lower laminae that are composed of the same material that is present within Laminate A; however, the inner (core) lamina of Laminate C is composed of a material that is similar to a typical unidirectional carbon fiber reinforced polymer having its fibers oriented perpendicular to the longitudinal axis of the beam, but with a shear modulus set an order of magnitude lower than typical materials of this type. The three laminates are summarized in Table 2.

**Table 2.** Example laminates presented in this manuscript

	Laminate A	Laminate B	Laminate C
Lamina 3	Carbon $0^\circ$ $E_{xx} = 119000 \text{ N/mm}^2$ $G_{xz} = 4230 \text{ N/mm}^2$ Thickness = 1 mm	Carbon $0^\circ$ $E_{xx} = 119000 \text{ N/mm}^2$ $G_{xz} = 4230 \text{ N/mm}^2$ Thickness = 1 mm	Carbon $0^\circ$ $E_{xx} = 119000 \text{ N/mm}^2$ $G_{xz} = 4230 \text{ N/mm}^2$ Thickness = 1 mm
Lamina 2	Carbon $0^\circ$ $E_{xx} = 119000 \text{ N/mm}^2$ $G_{xz} = 4230 \text{ N/mm}^2$ Thickness = 1 mm	Carbon $90^\circ$ $E_{xx} = 9270 \text{ N/mm}^2$ $G_{xz} = 3228 \text{ N/mm}^2$ Thickness = 1 mm	Modified Carbon $90^\circ$ $E_{xx} = 9270 \text{ N/mm}^2$ $G_{xz} = 323 \text{ N/mm}^2$ Thickness = 1 mm
Lamina 1	Carbon $0^\circ$ $E_{xx} = 119000 \text{ N/mm}^2$ $G_{xz} = 4230 \text{ N/mm}^2$ Thickness = 1 mm	Aluminium $E_{xx} = 68900 \text{ N/mm}^2$ $G_{xz} = 26200 \text{ N/mm}^2$ Thickness = 1 mm	Carbon $0^\circ$ $E_{xx} = 119000 \text{ N/mm}^2$ $G_{xz} = 4230 \text{ N/mm}^2$ Thickness = 1 mm

As a comparison with the present beam theory, the beam loading configuration and the three laminates discussed were also analyzed using an Euler-Bernoulli beam model, a Timoshenko beam model, and a Zigzag beam model, wherein said Zigzag beam model utilized the HLMZFS procedure<sup>24</sup> in order to partition each lamina into 64 laminae.

The section constants calculated for each beam configuration are given in Table 3. It should be noted that the values of  $\Lambda_{xz}$  used for the present beam model differ from the values of  $\kappa_z AG_{xz}$  used for the Timoshenko beam model. The values of  $\Lambda_{xz}$  used for the present beam model were calculated in accordance with the method presented in Section 4.3. Conversely, the values of  $\kappa_z AG_{xz}$  used for the Timoshenko beam model were calculated using the “directional shear energy” method discussed in<sup>5</sup>, wherein shear strains were defined in terms of  $V_{zB_C}$  by substituting equation (8) into equation (26) or (27). It is worth noting that this “directional shear energy” method of calculating  $\kappa_z AG_{xz}$  constitutes a modified version of the method presented in<sup>7</sup>.

**Table 3.** Section constants for the example laminates presented in this manuscript

	Laminate A	Laminate B	Laminate C
$EI_{yy}$	267750.0 Nmm <sup>2</sup>	191600.7 Nmm <sup>2</sup>	258605.8 Nmm <sup>2</sup>
$\beta_{1z}$ (Present Beam Model)	3150.0 Nmm <sup>2</sup>	6095.3 Nmm <sup>2</sup>	17188.7 Nmm <sup>2</sup>
$\Lambda_{xz}$ (Present Beam Model)	10450.6 N	10481.5 N	1321.1 N
$\kappa_z AG_{xz}$ (Timoshenko Beam Model)	10575.0 N	10825.9 N	1415.1 N

As a further comparison with the present beam theory, the beam loading configuration and the three laminates discussed were also analyzed using the finite element method. NX NASTRAN<sup>38</sup> was used for this analysis. The beams were analyzed using two-dimensional shell elements (CQUAD4) and two-dimensional orthotropic (MAT8) material cards. The mesh was a rectangular grid having a uniform spacing of 0.1 mm. All of the nodes were constrained to remain within the loading plane. Each of the nodes at the support ( $x = 12 \text{ mm}$ ) was restrained against translation

in the  $z$  direction using a single-point constraint (SPC). All of the nodes at the plane of symmetry ( $x = 0$  mm) were connected to a common central node (independent node) using a rigid body element (RBE2); a transverse force was applied to the common central node (independent node) of this rigid body element (RBE2), wherein said transverse force had a magnitude of 100 N (half of the total load), and was applied parallel to the  $z$ -axis. In addition, each of the nodes at the plane of symmetry ( $x = 0$  mm) was restrained against translation in the  $x$  direction using a grounded spring element (CBUSH) with a very high translational stiffness in the  $x$  direction. Since all of the beam models discussed herein assume that  $\epsilon_z \approx 0$ , where  $\epsilon_z$  is the normal strain that acts parallel to the  $z$ -axis, each material, except aluminium, was assigned a very high elastic modulus parallel to the  $z$ -axis ( $E_{zz} = 927000.0$  N/mm<sup>2</sup>), and each material was assigned a Poisson's ratio of zero. In the case of the aluminium material, an isotropic material model was used. The deformed shapes of the three finite element models are shown in Figure 3, Figure 4, and Figure 5. Readers who wish to reproduce this analysis are directed to the NX NASTRAN input and output files that the authors have provided in an online archive<sup>37</sup>.

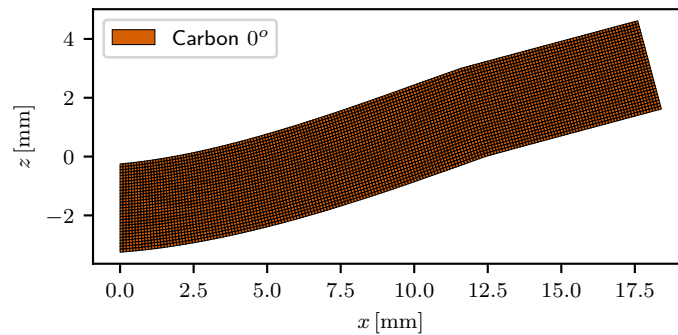


**Figure 3.** Deformed shape of the finite element model of the beam comprising Laminate A. The deformation has been scaled by a factor of 10

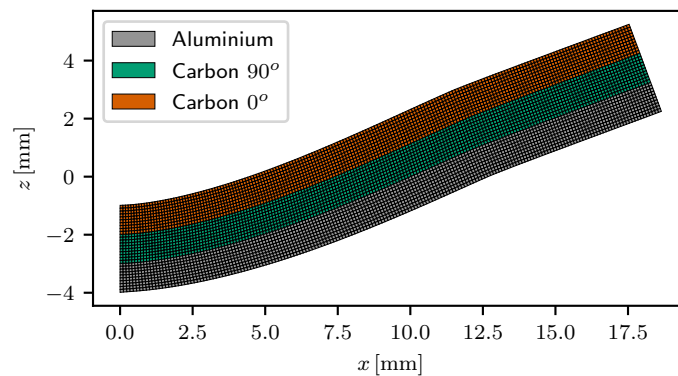


**Figure 4.** Deformed shape of the finite element model of the beam comprising Laminate B. The deformation has been scaled by a factor of 10

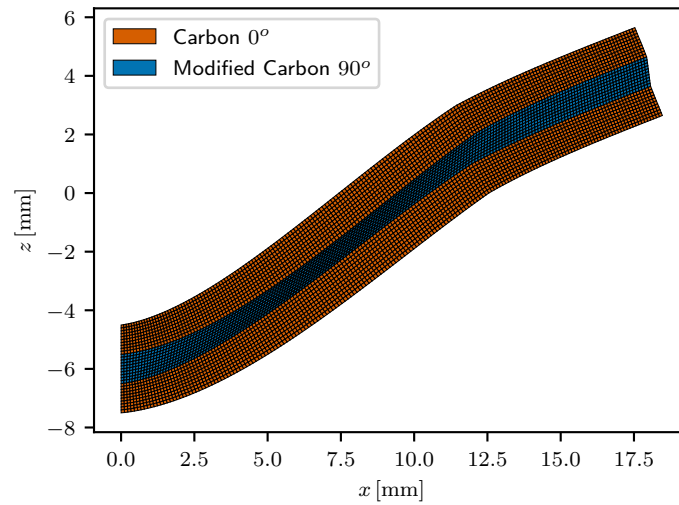


**Figure 5.** Deformed shape of the finite element model of the beam comprising Laminate C. The deformation has been scaled by a factor of 10

The following discussion utilizes various plots to compare the analytical results of the various models discussed herein. In the interest of brevity, these plots abbreviate the various models as follows: the Euler-Bernoulli beam model is denoted by “Euler-Bernoulli”, the Timoshenko beam model is denoted by “Timoshenko”, the Zigzag beam model with the HLMZFS procedure is denoted by “Zigzag”, the finite element model is denoted by “FEM”, and the present beam model is denoted by “Present Model”.

The transverse deflections,  $w$ , predicted by each model are shown in Figure 6, Figure 7, and Figure 8. For each of the finite element models, the transverse deflection at each position along the  $x$ -axis is taken as the mean of the  $z$  displacements of all of the nodes that are present at that  $x$  position. From examining Figure 6 and Figure 7, it is evident that the present beam model, the Timoshenko beam model, and the Zigzag beam model all exhibit strong agreement with the results of the finite element analyses of the beams comprising Laminate A and Laminate B. This can be attributed to the relatively modest shear deformation, as well as the relatively modest shear-warping stiffness associated with these beam configurations. The beam comprising Laminate C exhibits significantly greater shear compliance coupled with significantly greater shear-warping stiffness (as summarized in Table 3); Figure 8 shows that the Timoshenko beam model over-predicts the transverse deflections while the present beam model slightly underpredicts the transverse deflections. Additionally, outside the loaded span (for  $x > 12$  mm), the Timoshenko beam model matches the prediction of the Euler-Bernoulli beam model, while the present beam model and the Zigzag beam model both follow the prediction of the finite element model much more closely.

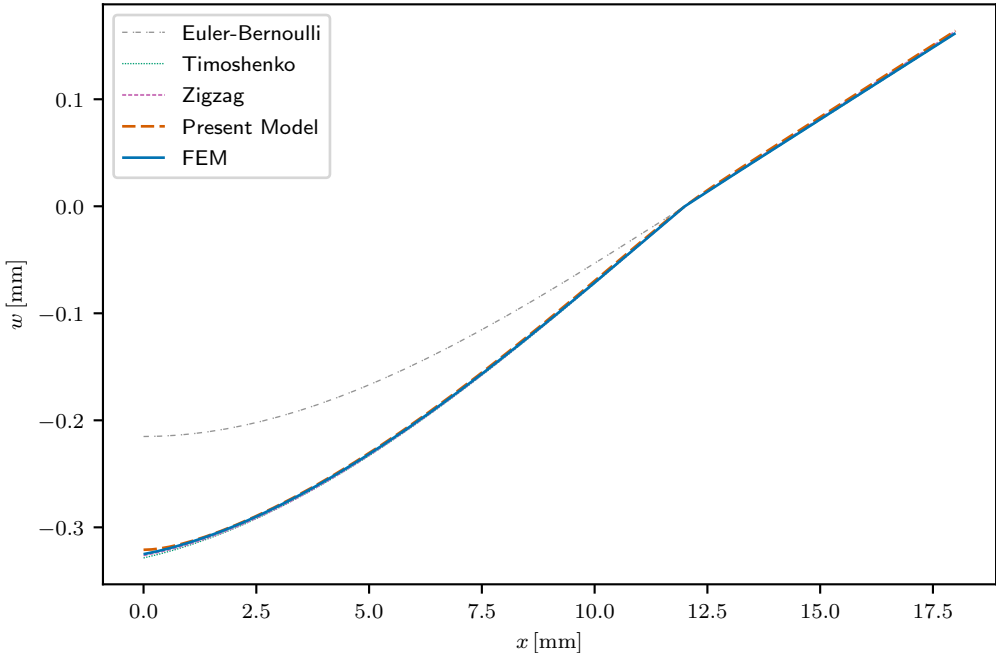


Figure 6. Transverse deflections of the beam comprising Laminate A, predicted by various models

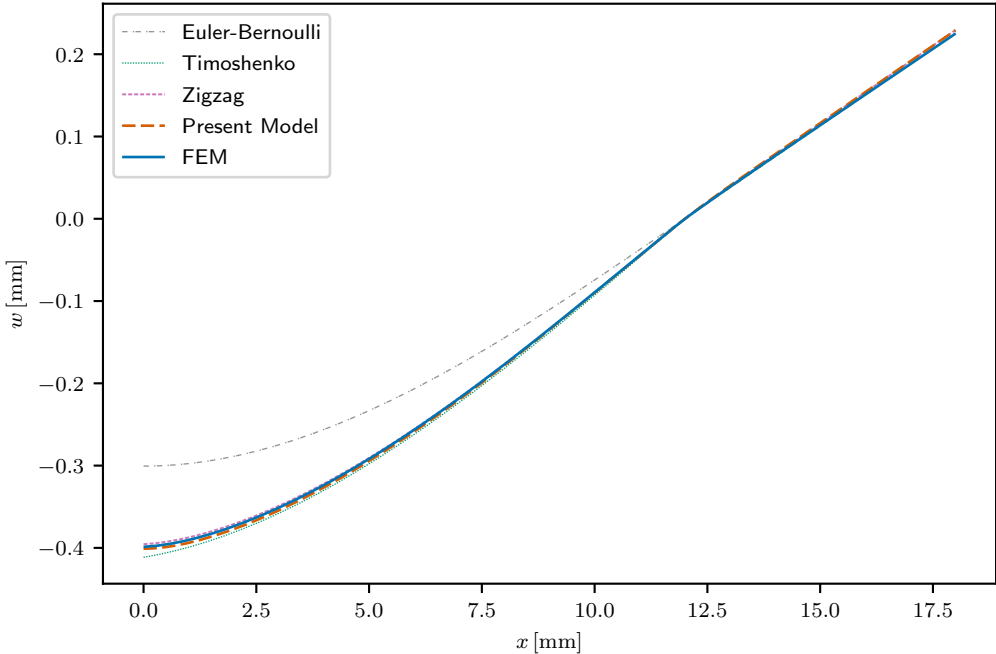
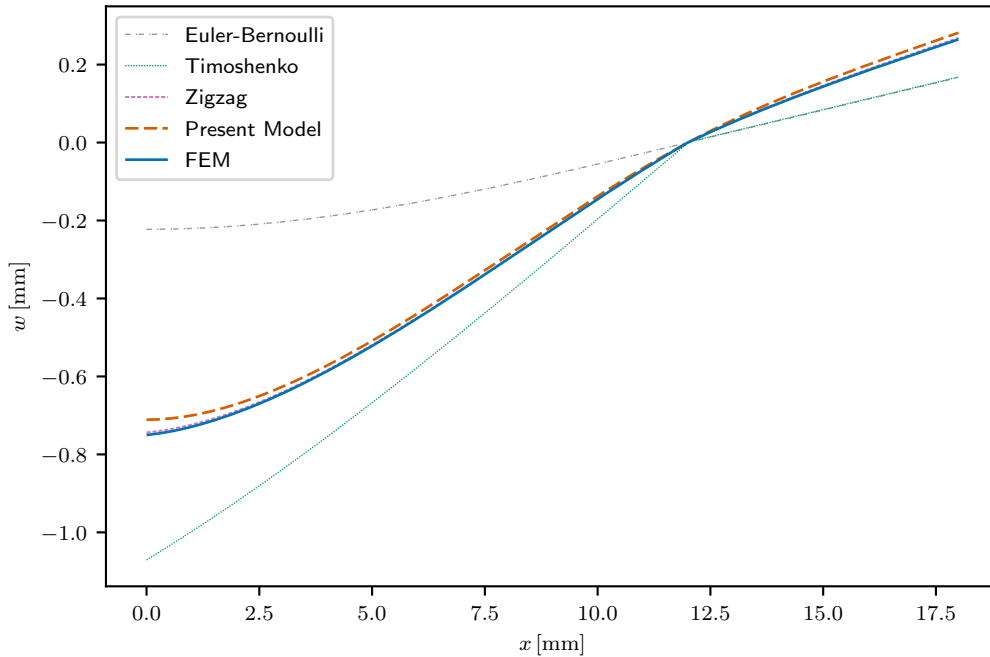
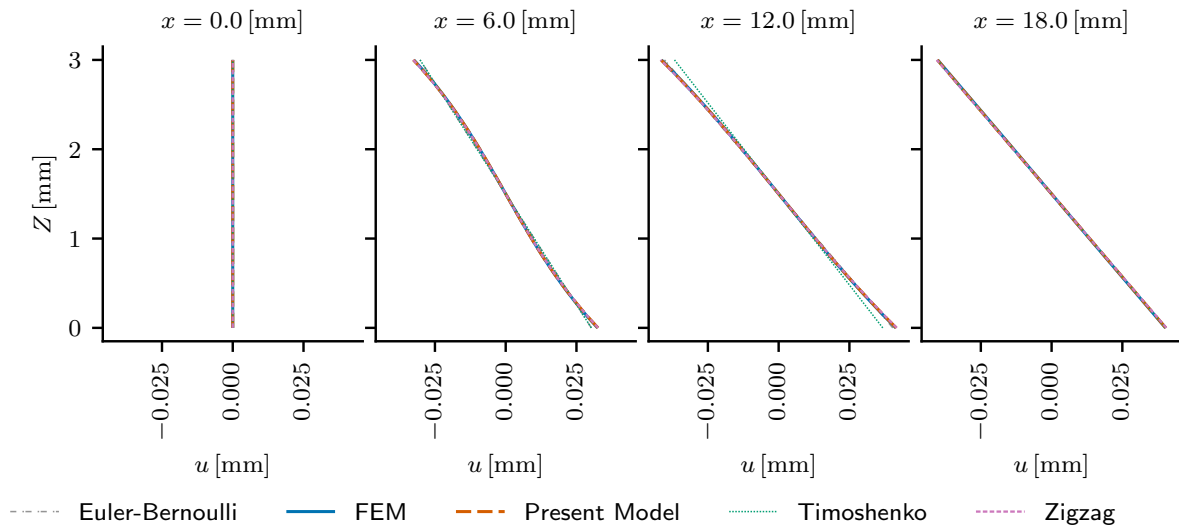


Figure 7. Transverse deflections of the beam comprising Laminate B, predicted by various models



**Figure 8.** Transverse deflections of the beam comprising Laminate C, predicted by various models

The longitudinal displacements,  $u$ , predicted by each model are shown in Figure 9, Figure 10, and Figure 11. In the present beam model,  $u = u_B + u_{W1}$ . The longitudinal displacements are plotted at the plane of symmetry ( $x = 0$  mm), midway between the plane of symmetry and the support ( $x = 6$  mm), at the support ( $x = 12$  mm), and at the free end of the beam ( $x = 18$  mm). The warping of the section is particularly evident for the beam comprising Laminate C, as the shear deformation of that beam is considerable.



**Figure 9.** Longitudinal displacements within the beam comprising Laminate A, predicted by various models at various positions along the length of the beam

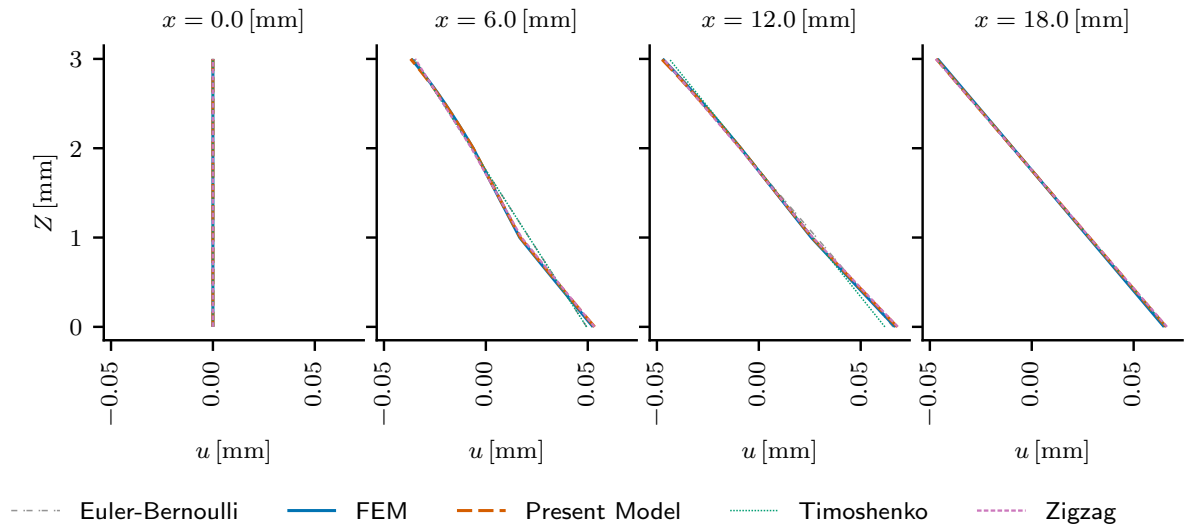


**Figure 10.** Longitudinal displacements within the beam comprising Laminate B, predicted by various models at various positions along the length of the beam

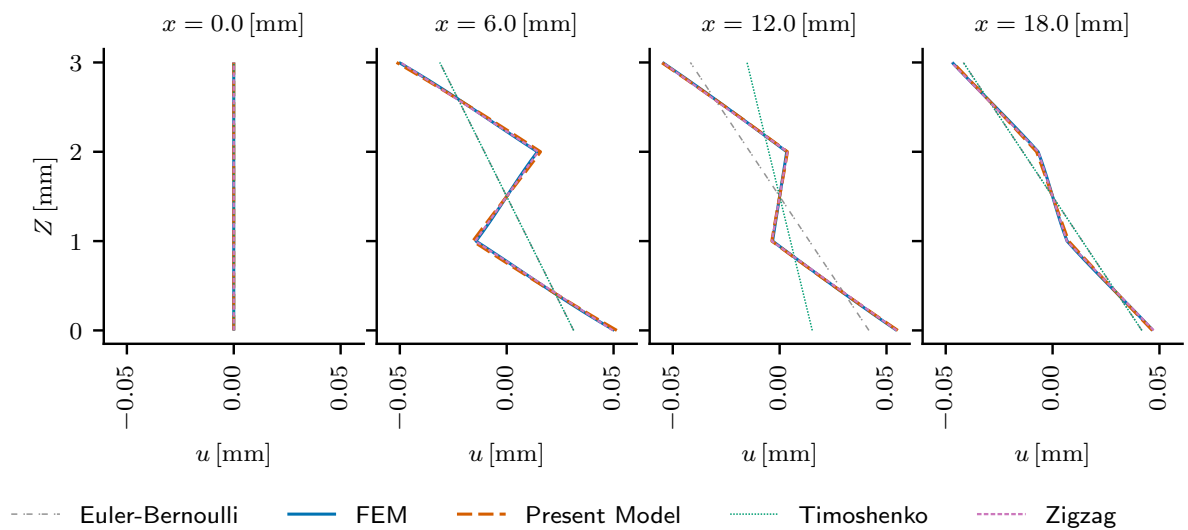


**Figure 11.** Longitudinal displacements within the beam comprising Laminate C, predicted by various models at various positions along the length of the beam

The longitudinal normal stress distributions,  $\sigma_x$ , predicted by each model are shown in Figure 12, Figure 13, and Figure 14. The longitudinal normal stress distributions are plotted adjacent the plane of symmetry ( $x = 0.5$  mm), midway between the plane of symmetry and the support ( $x = 6$  mm), adjacent the support ( $x = 11.5$  mm and  $x = 12.5$  mm), midway between the support and the free end of the beam ( $x = 15$  mm), and at the free end of the beam ( $x = 18$  mm). In the case of the beam comprising Laminate A, the present beam model tends to over-predict the non-linearity of the longitudinal normal stresses near shear force discontinuities, such as those found at the plane of symmetry (where the shear force changes signs) and at the support (where the shear force changes from a non-zero value to zero). In the case of the beam comprising Laminate B, the present beam model exhibits relatively strong agreement with the results of the finite element analysis at all of the investigated positions, while the Zigzag beam model exhibits moderate agreement with the results of the finite element analysis, and the other models exhibit

relatively poor agreement with the results of the finite element analysis. In the case of the beam comprising Laminate C, the present beam model and the Zigzag beam model both exhibit relatively strong agreement with the results of the finite element analysis at all of the investigated positions, while the other models exhibit relatively poor agreement with the results of the finite element analysis.

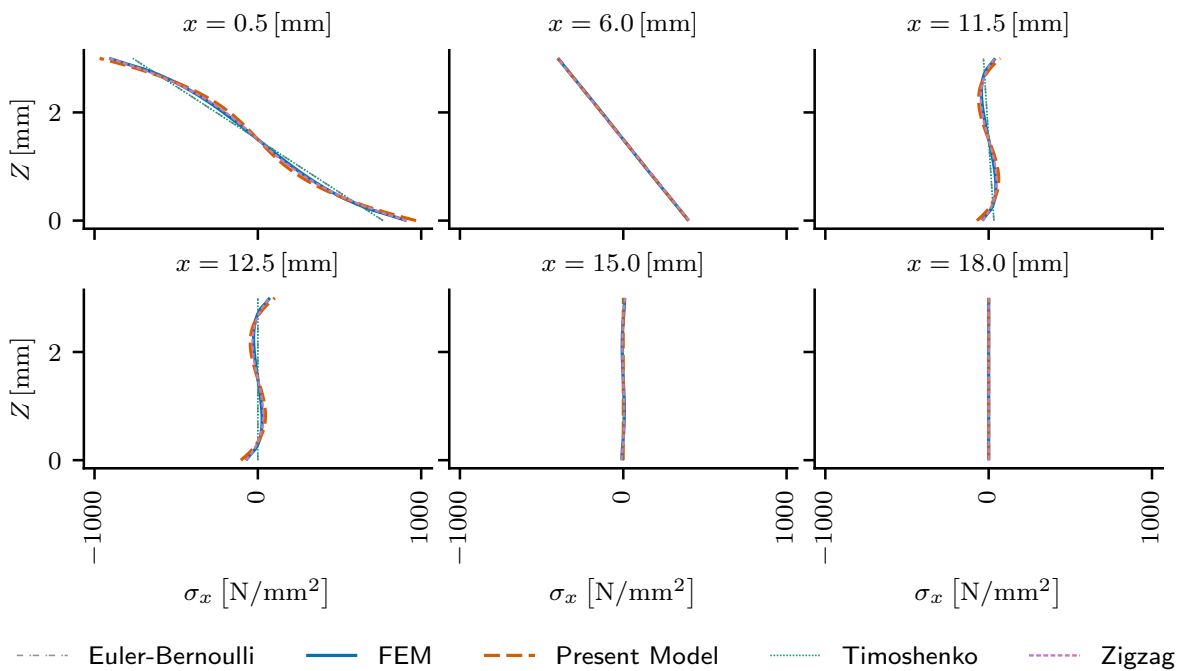


**Figure 12.** Longitudinal normal stress distribution through the thickness of the beam comprising Laminate A, predicted by various models at various positions along the length of the beam

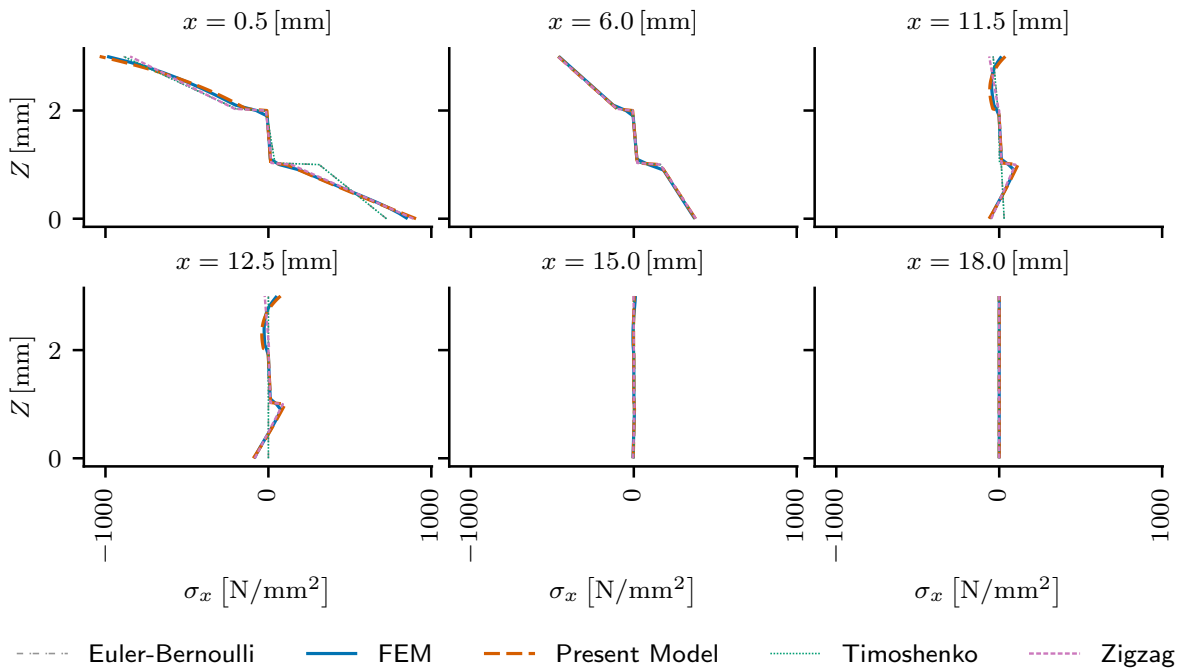


**Figure 13.** Longitudinal normal stress distribution through the thickness of the beam comprising Laminate B, predicted by various models at various positions along the length of the beam

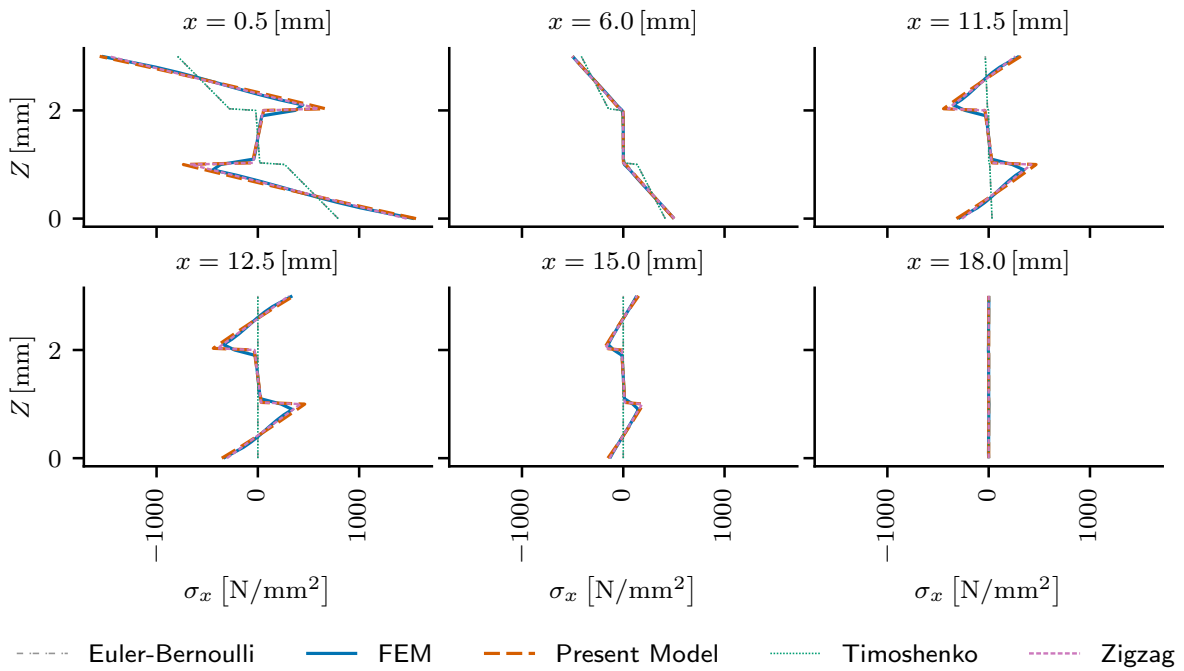


**Figure 14.** Longitudinal normal stress distribution through the thickness of the beam comprising Laminate C, predicted by various models at various positions along the length of the beam

The shear stress distributions,  $\tau_{xz}$ , predicted by each model are shown in Figure 15, Figure 16, and Figure 17. The shear stress distributions are plotted adjacent the plane of symmetry ( $x = 0.5$  mm), midway between the plane of symmetry and the support ( $x = 6$  mm), adjacent the support ( $x = 11.5$  mm and  $x = 12.5$  mm), midway between the support and the free end of the beam ( $x = 15$  mm), and at the free end of the beam ( $x = 18$  mm). In the case of the beam comprising Laminate A, the Zigzag beam model exhibits relatively strong agreement with the results of the finite element analysis at all of the investigated positions, though the shear stresses do not vanish at the surfaces of the beam. In the case of the beam comprising Laminate A, the present beam model tends to over-predict the non-uniformity of the through-thickness shear stress distribution near shear force discontinuities, such as those found at the plane of symmetry (where the shear force changes signs) and at the support (where the shear force changes from a non-zero value to zero). In the cases of the beams comprising Laminate B and Laminate C, the present beam model exhibits relatively strong agreement with the results of the finite element analysis at all of the investigated positions, while the Zigzag beam model exhibits moderate agreement with the results of the finite element analysis, and the other models exhibit relatively poor agreement with the results of the finite element analysis.

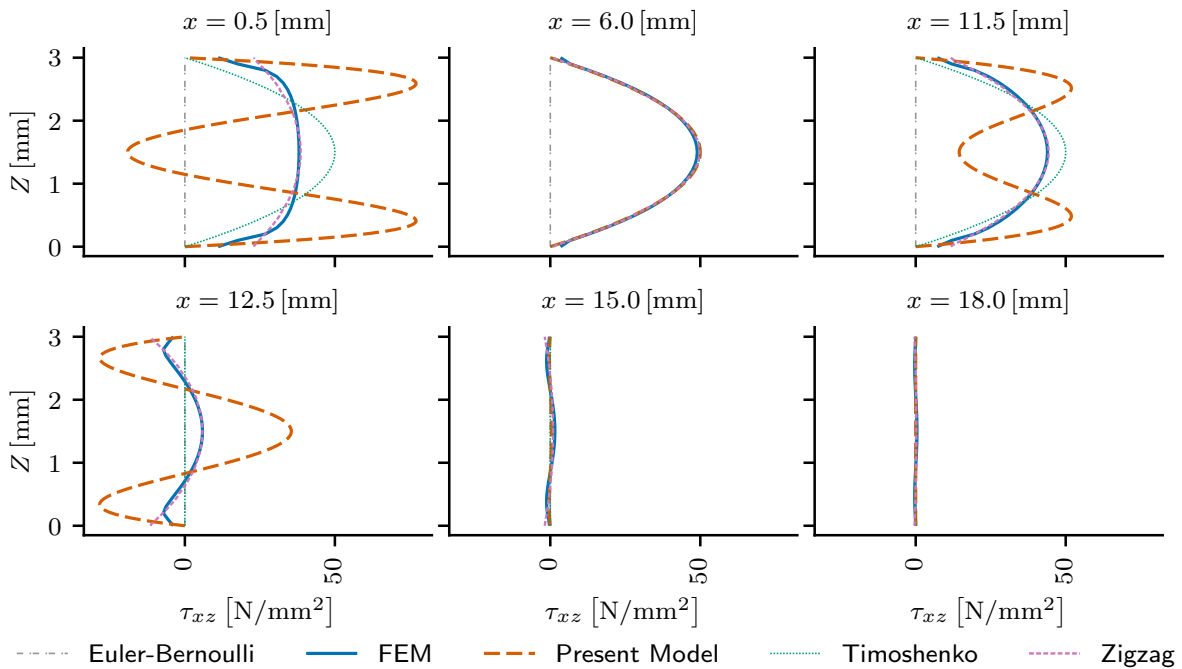


**Figure 15.** Shear stress distribution through the thickness of the beam comprising Laminate A, predicted by various models at various positions along the length of the beam

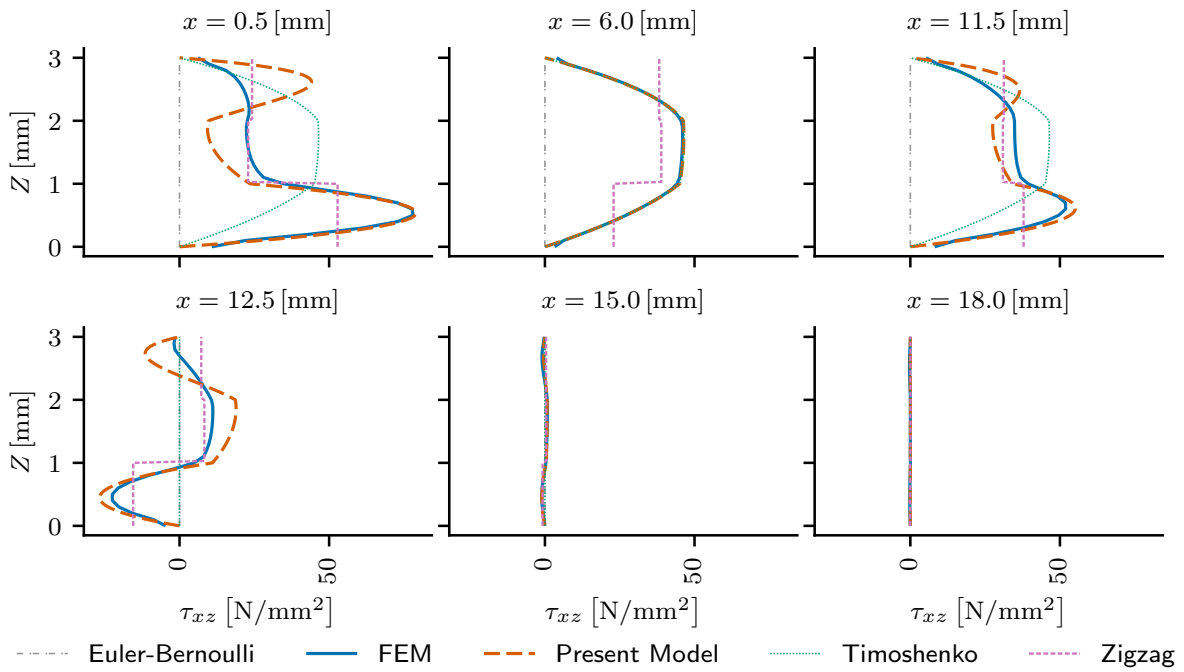


**Figure 16.** Shear stress distribution through the thickness of the beam comprising Laminate B, predicted by various models at various positions along the length of the beam

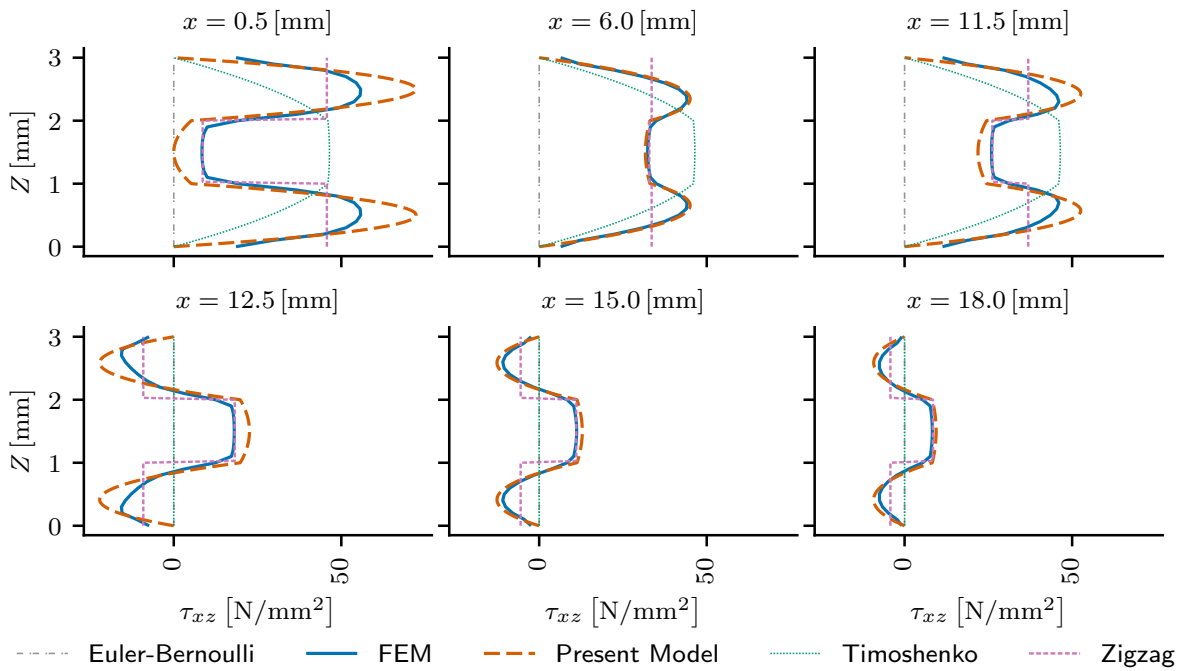


**Figure 17.** Shear stress distribution through the thickness of the beam comprising Laminate C, predicted by various models at various positions along the length of the beam

The inaccuracy of the present beam model's stress predictions in the vicinity of shear force discontinuities can likely be attributed to the order of the governing differential equations of the model. In each of Laminate B and Laminate C, any two adjacent laminae exhibit significantly different mechanical properties. The shear-warping displacement fields of the beams comprising Laminate B and Laminate C are heavily influenced by the heterogeneity of these laminates, and the influence of this heterogeneity is substantially represented by the component of the shear-warping displacement field that corresponds to the  $M_{yyw_1}$  and  $V_{zw_1c}$  terms of the governing differential equations of the present beam model. Heterogeneous beams (such as those comprising Laminate B or Laminate C) are indeed influenced by higher-order shear-warping effects; however, the authors believe that this influence is relatively minor in comparison with the influence of the effects that correspond to the  $M_{yyw_1}$  and  $V_{zw_1c}$  terms of the governing differential equations of the present beam model. Conversely, in the case of a homogeneous beam (such as the beam comprising Laminate A), the authors believe that the shear-warping displacement field exhibits non-trivial contributions from higher-order shear-warping effects that are not represented by the component of the shear-warping displacement field that corresponds to the  $M_{yyw_1}$  and  $V_{zw_1c}$  terms of the governing differential equations of the present beam model. If it were necessary to achieve accurate stress predictions at all positions within a homogeneous beam (such as the beam comprising Laminate A), then it would likely be necessary to introduce higher-order terms to the governing differential equations of the model, as discussed in Section 6.

Notwithstanding the foregoing, the reader will appreciate that, although the fidelity of the stress predictions of the present beam model appear to be partially dependent upon the heterogeneity of the beam that is to be analyzed, the present beam model appears to offer accurate predictions of transverse deflections,  $w$ , irrespective of the composition of the beam that is to be analyzed.

## 9 Concluding Remarks

This manuscript presents a new higher-order beam model. The present beam model is governed by differential equations that are similar to those present in some existing higher-order beam models; however, the present beam model makes use of a novel method of calculating the transverse shear stiffness, which facilitates the calculation of a shear-warping stiffness without the need for an assumed warping displacement field, and without introducing any additional kinematic variables. Comparisons with the results of finite element analyses suggest that the present beam model is able to accurately represent the deformation of beams that exhibit non-trivial shear compliance as well as non-trivial shear-warping stiffness. It was also shown that the present beam model facilitates the recovery of the distributions of longitudinal normal stresses and transverse shear stresses. These stress distribution predictions are generally more accurate than those calculated using Euler-Bernoulli or Timoshenko beam theories. In the case of heterogeneous laminated composite beams, the present beam model offers stress distribution predictions that are slightly more accurate than those offered by zigzag models; however, in the case of a homogeneous beam, it was shown that the present beam model gives some erroneous stress predictions in vicinities where the transverse shear force distribution exhibits a discontinuity. The authors postulate that the governing equations of the present beam model constitute the first few terms of an infinite series, and it is suggested that the fidelity of the present beam model can likely be improved by continuing the development of said hypothetical infinite series, thus adding higher-order terms to the governing equations.

### Acknowledgements

Not applicable.

### Declaration of conflicting interests

Not applicable.

### Funding

Not applicable.

### Supplemental material

The authors have provided an online archive<sup>37</sup>, which includes the Python source code for the computer software that was used to solve the present beam model, as well as the NX NASTRAN input and output files corresponding to the finite element analyses that are discussed herein.

## References

1. Timoshenko S. On the correction for shear of the differential equation for transverse vibrations of prismatic bars. *Philosophical Magazine* 1921; 41: 744–746.
2. Timoshenko S. On the transverse vibrations of bars of uniform cross-section. *Philosophical Magazine* 1922; 43: 125–131.
3. Augarde C and Deeks A. The use of Timoshenko's exact solution for a cantilever beam in adaptive analysis. *Finite Elements in Analysis and Design* 2008; 44(9-10): 595–601. <https://doi.org/10.1016/j.finel.2008.01.010>.
4. Sapountzakis E and Argyridi A. Literature overview of higher order beam theories taking into account in-plane and out-of-plane deformation. *Journal of Advances in Civil Engineering and Construction Materials* 2018; 1(1): 1–15.
5. Dong S, Alpdogan C and Taciroglu E. Much ado about shear correction factors in Timoshenko beam theory. *International Journal of Solids and Structures* 2010; 47(13): 1651–1665. <https://doi.org/10.1016/j.ijsolstr.2010.02.018>.
6. Cowper G. The shear coefficient in Timoshenko's beam theory. *Journal of Applied Mechanics* 1966; 33(2): 335–340. <https://doi.org/10.1115/1.3625046>.
7. Renton J. Generalized beam theory applied to shear stiffness. *International Journal of Solids and Structures* 1991; 27(15): 1955–1967. [https://doi.org/10.1016/0020-7683\(91\)90188-L](https://doi.org/10.1016/0020-7683(91)90188-L).
8. Yu W, Volovoi V, Hodges D et al. Validation of the Variational Asymptotic Beam Sectional analysis (VABS). *American Institute of Aeronautics and Astronautics (AIAA) Journal* 2002; 40(10): 2105–2113. <https://doi.org/10.2514/2.1545>.
9. Yu W, Hodges D, Volovoi V et al. A generalized Vlasov theory for composite beams. *Thin-Walled Structures* 2005; 43(9): 1493–1511. <https://doi.org/10.1016/j.tws.2005.02.003>.
10. Yu W, Hodges D and Ho J. Variational asymptotic beam sectional analysis - An updated version. *International Journal of Engineering Science* 2012; 59: 40–64. <https://doi.org/10.1016/j.ijengsci.2012.03.006>.
11. Dong S, Kosmatka J and Lin H. On Saint-Venant's problem for an inhomogeneous, anisotropic cylinder - Part I: Methodology for Saint-Venant solutions. *Journal of Applied Mechanics* 2001; 68(3): 376–381. <https://doi.org/10.1115/1.1363598>.
12. Kosmatka J, Lin H and Dong S. On Saint-Venant's problem for an inhomogeneous, anisotropic cylinder - Part II: Cross-sectional properties. *Journal of Applied Mechanics* 2001; 68(3): 382–391. <https://doi.org/10.1115/1.1365152>.
13. Lin H, Dong S and Kosmatka J. On Saint-Venant's problem for an inhomogeneous, anisotropic cylinder - Part III: End effects. *Journal of Applied Mechanics* 2001; 68(3): 392–398. <https://doi.org/10.1115/1.1363597>.
14. Lin H and Dong S. On the Almansi-Michell problems for an inhomogeneous, anisotropic cylinder. *Journal of Mechanics* 2006; 22(1): 51–57. <https://doi.org/10.1017/S1727719100000782>.
15. El Fatmi R and Zenri H. On the structural behavior and the Saint Venant solution in the exact beam theory: Application to laminated composite beams. *Computers and Structures* 2002; 80(16-17): 1441–1456. [https://doi.org/10.1016/S0045-7949\(02\)00090-1](https://doi.org/10.1016/S0045-7949(02)00090-1).
16. El Fatmi R and Zenri H. A numerical method for the exact elastic beam theory. Applications to homogeneous and composite beams. *International Journal of Solids and Structures* 2004; 41(9-10): 2521–2537. <https://doi.org/10.1016/j.ijsolstr.2003.12.011>.
17. El Fatmi R. Non-uniform warping including the effects of torsion and shear forces. Part I: A general beam theory. *International Journal of Solids and Structures* 2007; 44(18-19): 5912–5929. <https://doi.org/10.1016/j.ijsolstr.2007.02.006>.
18. El Fatmi R. Non-uniform warping including the effects of torsion and shear forces. Part II: Analytical and numerical applications. *International Journal of Solids and Structures* 2007; 44(18-19): 5930–5952. <https://doi.org/10.1016/j.ijsolstr.2007.02.005>.
19. Chakravarty U. *Section Builder: A Finite Element Tool for Analysis and Design of Composite Beam Cross-Sections*. Ph.D Thesis, Georgia Institute of Technology, North Avenue, Atlanta, Georgia, 30332, USA, 2008.
20. Shi G and Voyiadjis G. A sixth-order theory of shear deformable beams with variational consistent boundary conditions. *Journal of Applied Mechanics* 2011; 78(2): 021019. <https://doi.org/10.1115/1.4002594>.
21. Reddy J. A simple higher-order theory for laminated composite plates. *Journal of Applied Mechanics* 1984; 51(4): 745–752. <https://doi.org/10.1115/1.3167719>.
22. Cook G. A higher-order bending theory for laminated composite and sandwich beams. Contractor Report NASA/CR-201674, National Aeronautics and Space Administration, Langley Research Center, Hampton, Virginia, 23681-0001, USA, 1997.
23. Abadikhah H. *Higher Order Beam Equations*. Master's Thesis, Chalmers University of Technology, SE-412 96 Göteborg, Sweden, 2011. ISSN 1652-8557.
24. Tessler A, Di Sciuva M and Gherlone M. Refined zigzag theory for homogeneous, laminated composite, and sandwich plates: A homogeneous limit methodology for zigzag function selection. Technical Publication NASA/TP-2010-216214, National Aeronautics and Space Administration, Langley Research Center, Hampton, Virginia, 23681-2199, USA, 2010.

25. Tessler A, Di Sciuva M and Gherlone M. Refinement of Timoshenko beam theory for composite and sandwich beams using zigzag kinematics. Technical Publication NASA/TP-2007-215086, National Aeronautics and Space Administration, Langley Research Center, Hampton, Virginia, 23681-2199, USA, 2007.
26. Schulze S, Pander M, Naumenko K et al. Analysis of laminated glass beams for photovoltaic applications. *International Journal of Solids and Structures* 2012; 49(15-16): 2027–2036. <https://doi.org/10.1016/j.ijsolstr.2012.03.028>.
27. Arya H, Shimpi R and Naik N. A zigzag model for laminated composite beams. *Composite Structures* 2002; 56(1): 21–24. [https://doi.org/10.1016/S0263-8223\(01\)00178-7](https://doi.org/10.1016/S0263-8223(01)00178-7).
28. Tessler A, Di Sciuva M and Gherlone M. A refined zigzag beam theory for composite and sandwich beams. *Journal of Composite Materials* 2009; 43(9): 1051–1081. <https://doi.org/10.1177/0021998308097730>.
29. Stamm K and Witte H. *Sandwichkonstruktionen - Berechnung, Fertigung, Ausführung*. Vienna, Austria: Springer-Verlag, 1974. ISBN 978-3-7091-8334-2, <https://doi.org/10.1007/978-3-7091-8334-2>.
30. Schwarze K. Numerische methoden zur berechnung von sandwichelementen. *Stahlbau* 1984; 53(12): 363–370. ISSN 0038-9145.
31. Carrera E and Giunta G. Refined beam theories based on a unified formulation. *International Journal of Applied Mechanics* 2010; 2(1): 117–143. <https://doi.org/10.1142/S1758825110000500>.
32. Carrera E, Giunta G and Petrolo M. *Developments and Applications in Computational Structures Technology*, chapter 4, A Modern and Compact Way to Formulate Classical and Advanced Beam Theories. Stirlingshire, United Kingdom: Saxe-Coburg Publications, 2010. pp. 75–112. <https://doi.org/10.4203/csets.25.4>.
33. Carrera E and Petrolo M. Refined beam elements with only displacement variables and plate/shell capabilities. *Meccanica* 2012; 47: 537–556. <https://doi.org/10.1007/s11012-011-9466-5>.
34. Carrera E, Cinefra M, Zappino E et al. *Finite Element Analysis of Structures Through Unified Formulation*. John Wiley & Sons Ltd., 2014. Print ISBN 9781119941217, Online ISBN 9781118536643, <https://doi.org/10.1002/9781118536643>.
35. Minera S, Patni M, Carrera E et al. Three-dimensional stress analysis for beam-like structures using Serendipity Lagrange shape functions. *International Journal of Solids and Structures* 2018; 141-142: 279–296. <https://doi.org/10.1016/j.ijsolstr.2018.02.030>.
36. Saint-Venant A. Mémoire sur la torsion des prismes. *Mémoires présentés par divers savants à l'Académie des Sciences* 1855; 14: 233–560.
37. Honickman H and Kloppenborg S. Supplemental material for the article entitled “A simple higher-order beam model that is represented by two kinematic variables and three section constants”, Version 1.1.0, 2020. Zenodo, DOI:10.5281/zenodo.4274199, <https://doi.org/10.5281/zenodo.4274199>.
38. Siemens Product Lifecycle Management Software Inc. NX Nastran 12.0.1. Computer Software, 2018.